

DisQ: A Markov Decision Process Based Language for Quantum Distributed Systems

LE CHANG, University of Maryland, USA

SAITEJ YAVVARI, Iowa State University, USA

RANCE CLEVELAND, University of Maryland, USA

SAMIK BASU, Iowa State University, USA

LIYI LI, Iowa State University, USA

The development of quantum computers has reached a great milestone, in spite of restrictions on important quantum resources: the number of qubits being entangled at a single-location quantum computer. Recently, there has been some work to combine single-location quantum computing and quantum networking techniques to develop distributed quantum systems such that large entangled qubit groups can be established through remote processors, and quantum algorithms can be executed distributively. We present DisQ as a framework to facilitate the rewrites of quantum algorithms to their distributed versions. The core of DisQ is a distributed quantum programming language that combines the concepts of Chemical Abstract Machine (CHAM) and Markov Decision Processes (MDP) with the objective of providing a clearly distinguishing quantum concurrent and distributed behaviors. Based on the DisQ language, we develop a simulation relation for verifying the equivalence of a quantum algorithm and its distributed versions. We present several case studies, such as quantum addition and Shor's algorithm, to demonstrate their equivalent rewrites to distributed versions.

1 Introduction

Quantum computing has shown a great potential for quantum advantage to program substantially faster algorithms compared to those written for classical computers, e.g., Shor's algorithm [Shor 1994] can factor a number in polynomial time – this problem is classically not known to be polynomial-time-computable. However, near-term intermediate-scale quantum (NISQ) computers have scalability challenges in executing practical quantum applications [Caleffi et al. 2022].

Quantum qubit entanglement, a major resource utilized in quantum algorithms, becomes the major bottleneck because a single-location NISQ computer usually has a fixed maximum of the allowed entangled qubit number due to machine limitations. For example, executing Shor's algorithm requires around 5,000 coherent and entangled qubits, while current single-location quantum computers can only support around 50 such qubits. Such limitations cannot be mitigated by single-location parallelism and concurrency. Hence, in recent years, quantum teleportation-based remote location quantum networking techniques have been explored to distributively execute quantum algorithms [Caleffi et al. 2022; Tang and Martonosi 2024]. These approaches aim to implement such strategies on real quantum hardware, ultimately leading to the formation of distributed quantum processors [Chen et al. 2023; Chu et al. 2024], confirmed by experimental results [Inc et al. 2024a; Main et al. 2024]; industries started the development of distributed quantum processors [IonQ 2024; Swayne 2024]. The key idea is combining the two techniques to create large entangled qubit groups and mitigate the scalability challenge with the cost of some manageable overheads. In addition, it is easier for a single quantum processor unit in this scheme to include different techniques to guarantee the qubit's correctness and reliability.

Existing quantum circuit-based programming languages [Feng et al. 2012; Gay and Nagarajan 2005; Ying and Feng 2009] focus on developing quantum parallelism and concurrency that can be used for simulating quantum distributed systems but do not explicitly support the specification of

the quantum distributed deployment mechanism. Simulating a quantum distributed system through a single-location quantum concurrency model may misrepresent some key features in combining the quantum circuit and networking techniques. For example, qubits in a single location cannot be a message transmitted to remote locations or manipulated by operations in remote locations, as the only way to communicate the information in these qubits is through quantum networking techniques. Moreover, the simulation relations in these frameworks are defined based on traditional deterministic bisimulation, which captures the probabilistic features in quantum programs through some quantum state representations, e.g., density matrices. Such simulations might not be practical in dealing with large quantum programs, as we need to show that a defined distributed quantum program must respect its original sequential program behavior.

To effectively translate sequential quantum programs into their distributed counterparts, we propose `DisQ`, a programming language framework inspired by the classical Chemical Abstract Machine (CHAM) [Berry and Boudol 1992]. `DisQ` allows for the definition, distinction, and analysis of both concurrent and remotely distributed quantum programs. `DisQ` utilizes the CHAM membrane concept to model remotely distributed quantum systems. Each membrane is a self-contained computation node, representing a single-location quantum computer. It may contain many processes that can share quantum resources and perform intra-location communication, having concurrent behaviors. Membranes can also perform inter-membrane communication with each other, with some constraints imposed for capturing the quantum distributed system behaviors i.e., the communication between two different membranes can be either through a quantum channel, the abstraction of remote Bell pair used in quantum teleportation to transmit quantum qubit information, or classical message communications, such as the ones in π -calculus [Milner et al. 1992].

To properly identify quantum qubit resources in intra- and inter- communications, where qubits can be shared among processes and can only be communicated through quantum channels among membranes, we include the locus concept [Li et al. 2024], a syntactic structure used to indicate a group of qubits possibly being entangled, allowing users to locally identify the qubits in a membrane while keeping other unrelated qubits invisible to the membrane, and permit the sharing of qubits among processes in a single membrane. The `DisQ` type system guarantees these properties.

We model the distributed quantum program semantics using a Markov Decision Process (MDP), where transition labels are assigned probability values, enabling the possibility to leverage traditional probabilistic simulation relations for reasoning about quantum programs. However, a significant challenge arises because different branches of the MDP may lead to the same states at measurement points. Hence, we propose a novel simulation relation that focuses on quantum measurements as critical sequence points, rather than equating step-by-step operational behaviors. In particular, we introduce the concept of simulation over pairs of sets of states, rather than individual states, providing a more comprehensive framework for validating the equivalence between a sequential quantum program and its distributed version.

`DisQ` aims to help rewrite sequential quantum programs to distributed ones, making executing non-trivial quantum programs possible in the near term. We have the following contributions.

- We develop `DisQ`, with its syntax and semantics, to capture both single-location quantum concurrency and remote-location distributed behaviors, where we impose proper conditions on the system to allow users to explore the boundaries of distributing quantum algorithms.
- The `DisQ` semantics is defined based on the combination of quantum system behaviors and traditional MDPs used for probabilistic programming. To the best of our knowledge, this is the first quantum program semantics based on traditional MDPs.
- Based on the locus concept, we develop a type system where the type soundness guarantees the deadlock freedom in the system as well as the proper classification between single and remote location communications.

- We develop a simulation relation to establish similarity between sequential and distributed quantum programs based on traditional MDP probabilistic simulations.
- We experiment with representative case studies, including quantum addition circuits and Shor’s algorithm, showing the utility of DisQ in analyzing sequential quantum programs and their distributed versions. Additionally, we show that DisQ can facilitate the cost evaluation of such distribution based on real-world quantum distributed computation models.

2 Background

Here, we provide background information on quantum computing, describing concurrent and distributed quantum systems. We show related works in Section 7.

Quantum Data. A quantum state (datum) ¹ consists of one or more quantum bits (*qubits*), which can be expressed as a two-dimensional vector $\begin{pmatrix} \alpha \\ \beta \end{pmatrix}$ where the *amplitudes* α and β are complex numbers s.t. $|\alpha|^2 + |\beta|^2 = 1$. We frequently write the qubit vector as $\alpha |0\rangle + \beta |1\rangle$ (the Dirac notation [Dirac 1939]), where $|0\rangle = \begin{pmatrix} 1 \\ 0 \end{pmatrix}$ and $|1\rangle = \begin{pmatrix} 0 \\ 1 \end{pmatrix}$ are *computational basis-kets*. When both α and β are non-zero, we can think of the qubit being “both 0 and 1 at once,” a.k.a. in a *superposition* [Nielsen and Chuang 2011], e.g., $\frac{1}{\sqrt{2}}(|0\rangle + |1\rangle)$ represents a superposition of $|0\rangle$ and $|1\rangle$. Larger quantum data can be formed by composing smaller ones with the *tensor product* (\otimes) from linear algebra. For example, the two-qubit datum $|0\rangle \otimes |1\rangle$ (also written as $|01\rangle$) corresponds to vector $[0\ 1\ 0\ 0]^T$. However, many multi-qubit data cannot be *separated* and expressed as the tensor product of smaller data; such inseparable quantum data are called *entangled*, e.g. $\frac{1}{\sqrt{2}}(|00\rangle + |11\rangle)$, known as a *Bell pair*. We can rewrite the Bell pair to $\sum_{b=0}^1 \frac{1}{\sqrt{2}} |bb\rangle$, where bb is a bit string consisting of two bits, each of which must be the same value (i.e., $b = 0$ or $b = 1$). Each term $\frac{1}{\sqrt{2}} |bb\rangle$ is named a *basis-ket* [Nielsen and Chuang 2011], consisting an amplitude ($\frac{1}{\sqrt{2}}$) and a basis $|bb\rangle$.

Quantum Computation and Measurement. Computation on a quantum datum consists of a series of *quantum operations*, each acting on a subset of qubits in the quantum datum. In the standard presentation, quantum computations are expressed as *circuits*, as shown in Figure 1, which depicts a circuit that prepares the Greenberger-Horne-Zeilinger (GHZ) state [Greenberger et al. 1989] – an n -qubit entangled datum of the form: $|\text{GHZ}^n\rangle = \frac{1}{\sqrt{2}}(|0\rangle^{\otimes n} + |1\rangle^{\otimes n})$, where $|d\rangle^{\otimes n} = \otimes_{j=0}^{n-1} |d\rangle$. In these circuits, each horizontal wire represents a qubit, and boxes on these wires indicate quantum operations, or *gates*. The circuit in Figure 1 uses n qubits and applies n gates: a *Hadamard* (H) gate and $n - 1$ *controlled-not* (CX) gates. Applying a gate to a quantum datum *evolves* it. Its traditional semantics is expressed by multiplying the datum’s vector form by the gate’s corresponding matrix representation: n -qubit gates are 2^n -by- 2^n matrices. Except for measurement gates, a gate’s matrix must be *unitary*, thus preserving appropriate invariants of quantum data’s amplitudes. A *measurement* (computational basis measurement) operation extracts classical information from a quantum datum. It collapses the datum to a basis state with a probability related to the datum’s amplitudes (*measurement probability*), e.g., measuring $\frac{1}{\sqrt{2}}(|0\rangle + |1\rangle)$ collapses the datum to $|0\rangle$ with probability $\frac{1}{2}$, and likewise for $|1\rangle$, returning classical value 0 or 1, respectively. A more general form of quantum measurement is *partial measurement*, which measures a subset of qubits in a qubit array; such operations often have simultaneity effects due to entanglement, i.e., in a Bell pair $\frac{1}{\sqrt{2}}(|00\rangle + |11\rangle)$, measuring one qubit guarantees the same outcome for the other – if the first bit is measured as 0, the second bit is too.

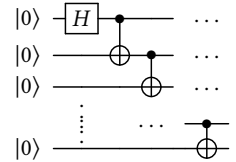


Fig. 1. GHZ Circuit

¹Most literature usually mentions quantum data as *quantum states*. In this paper, we refer to them as quantum data to avoid confusion between program and quantum states.

Quantum Concurrent, Networking, and Distributed Systems. Quantum networking techniques [Wehner et al. 2018] are developed for hybridizing the existing classical network infrastructure to construct the next generation of communication networks, a.k.a. quantum internet, featured with quantum mechanics [Granelli et al. 2022], which can provide more secure message communications than the existing infrastructure. Essentially, quantum networking techniques are based on quantum teleportation [Bennett et al. 1993; Rigolin 2005], where a Bell pair is viewed as quantum channels. The Bell pair circuit model (similar to the GHZ circuit above) serves as the theory basis of quantum channels while the real-world remote networking communication is based on more complicated networking techniques [Lago-Rivera et al. 2023; Pirandola et al. 2015; Shi and Qian 2020], different from the circuit-based quantum computing.

Quantum distributed computing utilizes quantum networking techniques to connect different single-location quantum computers to create a larger entanglement group, breaking the single-location computer entanglement scalability challenges [Padavic-Callaghan 2023], for executing comprehensive quantum algorithms in NISQ computers. The common ground of different proposals [Barral et al. 2024; Caleffi et al. 2022; Cuomo et al. 2020; Davarzani et al. 2022; DiAdamo et al. 2021; Häner et al. 2021; Inc et al. 2024b; Muralidharan 2024; Parekh et al. 2021; Tang and Martonosi 2024; Yimsiriwattana and Lomonaco Jr. 2004] is that the system connects different single-location quantum circuits, via remote location entanglement links, supported by quantum networking techniques. Other than the entanglement links, they ensure that the single-location machines and networking machines do not talk to each other, to keep each system self-closed to ensure the coherence of quantum qubits in different machines.

Quantum concurrent systems [Gheorghica 2023; Häner et al. 2022; Hillmich et al. 2020; Pysher et al. 2010] tried to utilize software and hardware multi-threaded techniques to improve the performance of executing quantum algorithms concurrently or parallelly. It is easy to confuse quantum concurrent and distributed systems. For example, [Meter and Devitt 2016] discussed how a quantum computer structure can be distributed to finish a task concurrently, and Beals et al. [2013] discussed how a single-location algorithm can be distributed to run in concurrent quantum systems. Because of the quantum decoherence limitations, single-location concurrent techniques might not achieve the goal of quantum distributed computing, so these two systems are different in the NISQ era. DISQ tries to capture the difference.

Markov Chains and Decision Processes. A Markov chain [Markov 1906, 1907] is a stochastic model describing a sequence of possible events in which the probability of each event depends only on the state attained in the previous event, and the probability of a program execution depends on the multiplication of the chain of the probabilities of events. It provides a standard labeled transition description of defining the semantic behaviors of probabilistic programming by viewing probabilistic as labels in semantic transitions; such labels are intrinsic and cannot be masked away. Markov decision process [Puterman 1994] extends a Markov chain by combining a nondeterministic choice with a probabilistic transition. Here, every step of computation is essentially a combination of two steps. We first make a nondeterministic choice—in DISQ, the choice is selecting membrane locations for an event happening—we then make a probabilistic move with a probability label.

3 Overview of Our Solution Strategy

Here, we present the features of DISQ and discuss the rationale behind them, followed by the necessity (and challenges) of describing a new equivalence relation to prove the correctness of constructing distributed quantum programs in DISQ with respect to their sequential version.

3.1 The CHAM Model and DISQ

The key feature of DISQ is its capability to model distributed quantum systems while explicitly representing the remote locations of subsystems. This allows for specifying both intra-location

(concurrent behaviors in a single location) and inter-location (distributed behaviors among remote locations) communication between subsystems. In light of this, the language is inspired by the *chemical abstract machine* (CHAM) description introduced by Berry and Boudol [Berry and Boudol 1992]. In the CHAM, the distributed and concurrent behaviors are modeled as chemical reactions between (abstract) molecules residing in a chemical solution that enables such reactions. The CHAM includes the concepts of *membranes* (or subsolutions), where the molecules inside the membranes can freely react; such behaviors correspond to concurrent behaviors. The reaction between molecules residing in two different membranes, corresponding to distributed behaviors, is allowed via a process referred to as *airlocking*. Intuitively, airlock allows for identifying and isolating a specific molecule in a membrane to get it ready for reaction with some other molecule (similarly airlocked) from a different membrane.

Classical Framework Level Interpretation. We first show a simple grammar containing only classical operations to highlight the distributed natural in the CHAM. In DisQ, we use the concept of membranes to express the grouping of distributed subsystems in different locations; that is, each membrane can be viewed as a quantum computer system at a particular location. We explicitly annotate the membranes with the location information to identify the locations of the quantum systems that are interacting with each other. Before formally introducing the language features of DisQ necessary for describing quantum systems, we first offer a gentle overview of its structure, incorporating membranes, airlock, and the standard process algebraic notion of concurrency (similar to π -calculus), to outline the salient features (and challenges) in developing DisQ. Consider a simple grammar for communicating processes with membranes:

$$R ::= 0 \mid D.R \qquad D ::= a!v \mid a?(y) \qquad P ::= \{\bar{R}\}_l \mid R\{\bar{T}\}_l$$

Here, a process of type R can be either a terminating process 0 or a sequential process where its behavior evolves by either performing a send-action ($a!v$: send v over channel a) or receive-action ($a?(y)$: receive some data over channel a and write to y). Two processes interact (synchronize) by sending and receiving messages over the same channel. The membrane description P is either a membrane $\{\cdot\}_l$ containing a multiset of processes of type R denoted by \bar{R} with explicit location information captured as l , or a membrane with an airlocked process $R\{\bar{T}\}_l$ where R is ready to interact with some other airlocked process associated with a different membrane. A DisQ program is a set of such membranes. Observe the inherent non-determinism in the interaction between processes within each membrane and between processes in different membranes. Any two processes in each membrane with appropriate send/receive actions may be non-deterministically selected for interaction; similarly, any two membranes with appropriate airlocked processes can be chosen for interactions across membranes. This is similar to the CHAM model.

Extending to Quantum. We augment the above basic actions with ones involving quantum operations as necessary (the DisQ syntax presented in Figure 5). Here, we focus on distributing the GHZ example in Section 2, with a single-location circuit $2n$ qubit GHZ program (n is of the order of 100), for qubit array $x[0, n]$ and $y[0, n]$ implementation as the follows.

$$x[0] \leftarrow H.x[0] \boxplus x[1] \leftarrow CX \dots x[n-1] \boxplus y[0] \leftarrow CX \dots y[n-2] \boxplus y[n-1] \leftarrow CX.0$$

Here, $s \leftarrow \mu$ denotes the application of the gate μ to the range s and \cdot is the sequence operator. If we view each membrane is a separate quantum processor, we can distribute the program to two parts, in two different membranes, containing the first and second half of the operations, to reduce the qubit numbers needed in each membrane. However, local qubits in a quantum processor, modeled by a membrane, cannot be transferred or referenced by another processor, and two processors require a quantum channel to communicate a qubit of information. Once a quantum channel is established, we can utilize quantum teleportation to transmit the qubit information from one to

the other. We will discuss the processes Te and Rt in Example 3.1 to illustrate the teleportation strategy. Using such a quantum channel, we can then distribute the above GHZ program at two locations l and r ; we will discuss this using the concept of membranes in Example 3.2.

Example 3.1 (Processes of Teleporation). We show the two processes of quantum teleportation, with example transitions in Appendix D.1. The $Te(s_1, s_2)$ and $Rt(s_3)$ processes below can be placed in two different membranes l and r , as it teleports the quantum information in s_1 to s_3 in the r membrane. The processes require s_2 and s_3 to refer to the same quantum channel. In DisQ , we require they have the same name.

$$\begin{aligned} Te(s_1, s_2) &= s_1 \boxplus s_2 \leftarrow \text{CX}. s_1 \leftarrow \text{H}. b_1 \leftarrow \mathcal{M}^i(s_1). b_2 \leftarrow \mathcal{M}^i(s_2). a!b_1. a!b_2. 0 \\ Rt(s_3) &= a?(b_1). a?(b_2). \text{if}(b_1) \{s_3 \leftarrow Z\}. \text{if}(b_2) \{s_3 \leftarrow X\}. 0 \end{aligned}$$

The two processes are executed in a DisQ program, $\{\{Te(s_1, s_2)\}\}_l, \{\{Rt(s_3)\}\}_r$, with s_2 and s_3 being an one qubit quantum channel. In l , the applications of CX and H gates encode the qubit s_1 with the channel s_2 , i.e., s_1, s_2 , become entangled. The two measurements (\mathcal{M}^i) divides the information in s_1 into two parts: b_1 and b_2 . These information are transferred via classical channels carrying the classical bits b_1 and b_2 . Further note, additional quantum information is passed along due to quantum entanglement (recall that s_2 and s_3 are the same quantum channel and s_1 and s_2 are entangled, i.e, s_3 is entangled as well). On receiving the two bits from membrane l , the membrane r restores the quantum information in s_1 by conditionally (depending on b_1 and b_2) applying Z and X to s_3 . After the process, s_3 has all the information in s_1 .

Example 3.2 (Distributed GHZ). We construct the GHZ state distributedly for the range $x[0, n)$ in membrane l and range $y[0, n)$ in membrane r . The two membranes' $c[0]$ qubits differ, but they refer to the same quantum channel.

$$\begin{aligned} R(j) = \text{if}(j+1 < n) \ x[j] \boxplus x[j+1] \leftarrow \text{CX}. R(j+1) \ \text{else} \ 0 \quad T(j) = \text{if}(j+1 < n) \ y[j] \boxplus y[j+1] \leftarrow \text{CX}. T(j+1) \ \text{else} \ 0 \\ \{x[0] \leftarrow \text{H}. R(0). Te(x[n-1], c[0])\}_l, \{Rt(c[0]). c[0] \boxplus y[0] \leftarrow \text{CX}. T(0). 0\}_r \end{aligned}$$

Observe that, the program syntax does not tell variable scopes and types. In addition, the teleportation is valid in Example 3.1 only if s_2 and s_3 are entangled and belong to a quantum channel, but the program syntax does not directly tell if the two $c[0]$ variables in the two membranes are entangled or not. This relies on an analysis to resolve the variable and entanglement scopes, which is captured by introducing 1) *loci* (κ) to group possibly entangled qubits, 2) standard *kind environments* (Ω) to record variable *kinds* (explained below) and scope for a membrane and 3) *locus type environments* (σ) to keep track of both loci and their quantum state types.

There are two kinds of data: scalar (C) and quantum ($\text{Q}(n)$, representing n qubit arrays). For simplicity, in a local membrane, we assume no aliasing in variable names and no overlapping between qubit arrays referred to by any two different variables; variables and locations are in distinct categories. The valuation of scalar kind data is either of type bitstrings (d) or natural numbers (n). On the other hand, quantum data valuations are represented using a varied Dirac notation $\sum_{j=0}^m z_j \beta_j \eta_j$, where m is the number of basis-kets in the quantum data. We *extend* the basis-ket structure, such that each basis-ket datum contains not only an amplitude z_j and a basis vector β_j , but also a frozen basis stack η_j , which stores basis vectors not directly involved in the current computation. The necessity for the frozen basis stack will be elaborated on later. The type of this quantum data describes how the qubit vectors relate to each other, introduced in Li et al. [2024]. This paper considers the most general type EN (entanglement).

A kind environment (Ω) classifies variables in a DisQ program as a classical or quantum kind. Quantum data are conceptually stored as a heap (a quantum state $\Phi \triangleq \bar{K} : q$), partitioned into regions described as loci (K) in DisQ ; each region contains possibly entangled qubits, with the guarantee that cross-locus qubits are not entangled. Each locus can be viewed as a chain of disjoint

Basic Terms:

Nat. Num	$m, n \in \mathbb{N}$	Bit	$b ::= 0 \mid 1$	Bitstring	$d \in b^+$	Variable/Classic Chan	x, y, a
Amplitude	$z \in \mathbb{C}$	Basis Vector	$\beta ::= (d\rangle)^*$	Location	l, r, u	Quantum Chan	c

Modes, Kinds, Types, and Classical/Quantum Data:

Kind	$g ::= \mathbb{C} \mid \mathbb{Q}(n)$
Classical Scalar Data	$v ::= d \mid n$
Frozen Basis Stack	$\gamma ::= (\beta\rangle)$
Full Basis Vector	$\eta ::= \beta\gamma$
Basic Ket	$w ::= z\eta$
Quantum Type	$\tau ::= \text{EN} \mid \dots$
Quantum Data	$q ::= \sum_{j=0}^m w_j$

Quantum Loci, Environment, and States

Qubit Array Range	$s ::= x[n, m]$	
Local Locus	$\kappa ::= \bar{s}$	concatenated op \sqcup
Locus	$K ::= \langle \kappa \rangle_l$	concatenated op \sqcup
Kind Environment	$\Omega ::= l \rightarrow x \rightarrow g$	
Local Type Environment	$\sigma ::= \bar{\kappa} : \bar{\tau}$	concatenated op \cup
Type Environment	$\Sigma ::= \bar{K} : \bar{\tau}$	concatenated op \cup
Local Quantum State (Heap)	$\varphi ::= \bar{\kappa} : \bar{q}$	concatenated op \cup
Quantum State (Heap)	$\Phi ::= \bar{K} : \bar{q}$	concatenated op \cup

Syntax Abbreviations and Basis/Locus Equations

$$\begin{aligned}
1\gamma \simeq \gamma \quad \sum_{j=0}^0 w_j \simeq w_0 \quad \sum_{j=0}^m w_j \simeq \sum_j w_j \quad z\beta(|\emptyset\rangle) \simeq z\beta \quad z\beta(|\beta'\rangle) \simeq z\beta\hat{\beta}' \quad x[n, n+1] \simeq x[n] \\
x[n, n] \equiv \emptyset \quad \emptyset \sqcup \kappa \equiv \kappa \quad |d_1\rangle |d_2\rangle \equiv |d_1 d_2\rangle \quad \langle q \sqcup q' \rangle_l \equiv \langle q \rangle_l \sqcup \langle q' \rangle_l \quad x[n, m] \equiv x[n, j] \sqcup x[j, m] \text{ if } j \in [n, m]
\end{aligned}$$

Fig. 2. DisQ data element. Each range $x[n, m]$ in a locus represents the number range $[n, m]$ in physical qubit array x . Loci are finite lists, while type environments and states are finite sets. The operations after "concatenated op" refer to the concatenation operations for loci, type environments, and quantum program states. Term a is no more than a variable, but we refer to it specifically for classical channels in this paper.

region segments labeled with explicit information about the location of local state variables, e.g., $\langle c[0] \rangle_l \sqcup \langle c[0] \rangle_r$ suggests that the two qubits, both named $c[0]$, in locations l and r are possibly entangled. Note that the l notation in loci captures location information.

In describing a local quantum state (φ) in a membrane, we disregard the location information; we can utilize local loci (κ) to refer to a quantum datum locally to a specific location. Each local locus consists a list of *disjoint ranges* (s), each represented by $x[n, m]$ —an in-place array slice selected from n to m (exclusive) in a physical qubit array x (always being Q kind). Ranges in a local locus are pairwise disjoint, written as $s_1 \sqcup s_2$. The quantum type of these quantum data describes their relationship and is denoted by $\Sigma \triangleq \bar{K} : \bar{\tau}$ associated with the corresponding valuations $\Phi \triangleq \bar{K} : \bar{q}$. We also include local type environments $\sigma \triangleq \bar{\kappa} : \bar{\tau}$ associated with the corresponding local valuations $\varphi \triangleq \bar{\kappa} : \bar{q}$, which forms the state at each location (referred to as a local state).

Figure 2 also presents some notational convenience (\simeq) and syntactic equivalences (\equiv), where \simeq is used for abbreviations. For instance, we abbreviate a singleton range $x[j, j+1]$ as $x[j]$; we omit the frozen basis stack notation ($|\cdot\rangle$) in a basis-ket presentation and **color** the frozen basis stack with a hat sign $\hat{\cdot}$, e.g., $\frac{1}{\sqrt{2}} |0\rangle \hat{1}$ means $\frac{1}{\sqrt{2}} |0\rangle (|\hat{1}\rangle)$; additionally, $\frac{1}{\sqrt{2}} |0\rangle \bar{1}$ means $\frac{1}{\sqrt{2}} |0\rangle |\bar{1}\rangle (|\emptyset\rangle)$.

Example 3.3 (Example Transitions). Below are the nondeterministic Transitions for Example 3.2 with $n > 2$; Omitted fragments are denoted by \dots . We use the $\langle \cdot \rangle_l$ structure in locus $\langle x[0, n] \rangle_l$ to indicate that the qubits in membrane l . We first apply a H operation to $x[0]$ in l in step (2), and then apply a CX to $\langle x[0] \sqcup x[1] \rangle_l$ in step (4), which is the application in step (4) (evolving from $R(0)$ to $R(1)$). Steps (1) and (3) rewrites the states to ideal forms. $\Phi = \{\langle c[0] \rangle_l \sqcup \langle c[0] \rangle_r : \sum_{j=0}^1 \frac{1}{\sqrt{2}} |j\rangle |j\rangle, \langle y[0, n] \rangle_r : |\bar{0}\rangle\}$.

- (1) $(\{\langle x[0, n] \rangle_l : \bar{0}\} \cup \Phi, \{x[0] \leftarrow H.R(0).Te(x[n-1], c[0])\}_l, \{\dots\}_r)$
- (2) $\equiv (\{\langle x[0] \rangle_l : |0\rangle, \langle x[1, n] \rangle_l : \bar{0}\} \cup \Phi, \{x[0] \leftarrow H.R(0).Te(x[n-1], c[0])\}_l, \{\dots\}_r)$
- (3) $\xrightarrow{L.1} (\{\langle x[0] \rangle_l : \sum_{j=0}^1 \frac{1}{2} |j\rangle, \langle x[1, n] \rangle_l : \bar{0}\} \cup \Phi, \{R(0).Te(x[n-1], c[0])\}_l, \{\dots\}_r)$
- (4) $\equiv (\{\langle x[0, 2] \rangle_l : \sum_{j=0}^1 \frac{1}{2} |j\rangle |0\rangle, \langle x[2, n] \rangle_l : \bar{0}\} \cup \Phi, \{R(0).Te(x[n-1], c[0])\}_l, \{\dots\}_r)$
- (5) $\xrightarrow{L.1} (\{\langle x[0, 2] \rangle_l : \sum_{j=0}^1 \frac{1}{2} |j\rangle |j\rangle, \langle x[2, n] \rangle_l : \bar{0}\} \cup \Phi, \{R(1).Te(x[n-1], c[0])\}_l, \{\dots\}_r)$

Here, locus $\langle c[0] \rangle_l \sqcup \langle c[0] \rangle_r$ indicates that the quantum channel $c[0]$ has two qubits in both membrane l and r and their quantum data might entangle with each other. The qubit order in a locus fixes the qubit basis-vector location, e.g., in line (4), the locus $\langle x[0, 2] \rangle_l$'s data, $\frac{1}{2}(\sum_{j=0}^1 |j\rangle |0\rangle)$, indicates that $x[0]$'s basis-vector refers to $|j\rangle$ and $x[1]$'s basis-vector refers to $|0\rangle$; thus, when we applying CX to $x[0] \sqcup x[1]$ (equivalence to $x[0, 2]$), it controls on the $|j\rangle$ to flip the bit in $|0\rangle$, for every j . We call the corresponding basis bits of qubits or locus fragments for a datum (or a basis-ket set) as the *qubit's/locus's position bases* of the datum (or the basis-ket set).

In the above transitions, we also perform state equivalence rewrites to rewrite the state in an ideal form for applications, e.g., line (2) cuts off locus $\langle x[0, n] \rangle_l$ (equivalence to $\langle x[0] \rangle_l \sqcup \langle x[1, n] \rangle_l$) to two loci $\langle x[0] \rangle_l$ and $\langle x[1, n] \rangle_l$, so the Hadamard applies to the first one. Line (4) takes the $x[1]$ qubit from the second locus to join the first one above. Such rewrites are type-guided in DisQ , i.e., we use the associated type environment to gear the quantum state rewrites because we require the type environment and quantum state always have the same domain; details are in Section 4.3.

Example 3.4 (Frozen Stack Example).

$$\frac{(\{c[0] : \sum_{j=0}^1 \frac{1}{2} |j\rangle \overline{|j\rangle}\}, c[0] \leftarrow X.0) \xrightarrow{1} (\{c'[0] \sqcup c[0] : \sum_{j=0}^1 \frac{1}{2} |\neg j\rangle \overline{|j\rangle}\}, 0)}{(\{\langle c[0] \rangle_l \sqcup \langle c[0] \rangle_r : \sum_{j=0}^1 \frac{1}{\sqrt{2}} |j\rangle |j\rangle\}, \{c[0] \leftarrow X.0\}_r) \xrightarrow{r.1} (\{\langle c[0] \rangle_l \sqcup \langle c[0] \rangle_r : \sum_{j=0}^1 \frac{1}{\sqrt{2}} |\neg j\rangle |j\rangle\}, \{0\}_r)}$$

We utilize locus structure to enable locality. In Example 3.4, locus $\langle c[0] \rangle_l \sqcup \langle c[0] \rangle_r$ contains qubits in membranes l and r , and we apply X gate to the locus locally in r , where we first localize the locus to focus on $c[0]$ in r . Consequentially, the locus' quantum data should only mention the part in r , and push the part in l to unreachable positions. The issue with dealing with quantum data is that it might contain entanglement, which makes individual qubit states inseparable. We utilize the frozen stack to hide the local unreachable qubit information. For example, the localization of the above locus does not mention the locus fragment $\langle c[0] \rangle_l$, as we push its position basis to the frozen stack of each basis-ket as $\overline{|j\rangle}$ and finishes the upper-level computation with the stack. Eventually, we retrieve the frozen position basis from the stack after the transition on the bottom.

3.2 Markov Decision Processes and DisQ

In DisQ , to capture the probabilistic nature of the quantum systems, we introduce and associate probabilities with the semantics of each interaction. Unlike the CHAM model, where all interactions are nondeterministic, in our case, the choice of the membrane is nondeterministic, while the interaction proceeding the choice is probabilistic (e.g., the choice of the process that evolves in the non-deterministically selected membrane is probabilistic). Hence, in the presence of both nondeterminism and probabilities, the semantics of systems described in our language DisQ is captured using Markov Decision Processes (MDP), where each evolution involves a nondeterministic

choice followed by a probabilistic move. Consider the following example evolution of a system described in DisQ with all classical operations:

$$\{\{a!v.0, 0\}\}_l, \{\{a?(y).0, 0\}\}_r \xrightarrow{l.\frac{1}{2}} a!v.0\{\{0\}\}_l, \{\{a?(y).0, 0\}\}_r \quad (1)$$

$$\xrightarrow{r.\frac{1}{2}} a!v.0\{\{0\}\}_l, a?(y).0\{\{0\}\}_r \quad (2)$$

$$\xrightarrow{l.r.1} \{\{0, 0\}\}_l, \{\{0, 0\}\}_r \quad (3)$$

$$\xrightarrow{l.1} \{\{0, 0\}\}_r \xrightarrow{r.1} \emptyset \quad (4)$$

There are two membranes at locations l and r , each containing two processes. Each step in the evolution includes a nondeterministic choice followed by a probabilistic one. For instance, in the first step (1), the nondeterministic choice results in the selection of membrane in location l (left membrane) followed by the probabilistic choice of airlocking the process $a!v.0$ in that membrane. This is presented in the annotation of the transition. Observe that, we have considered that selecting the processes in the left membrane is equally probable. Further, observe that there is another nondeterministic choice in selecting the membrane at location r . Proceeding further in the next step (2), we have considered a nondeterministic choice of selecting the membrane at location r followed by probabilistically selecting the process $a?(y).0$ to be airlocked. At this point, there are three nondeterministic choices: select the left membrane, select the right membrane, and select both membranes. The last choice is possible due to the presence of two airlocked processes in the membranes that are ready to interact. In Step (3), we show the third choice labeled as $l.r$ followed by the probability of interaction (in this case, the probability is 1 as there is exactly one probabilistic choice). In Step (3), we also implicitly present that the processes, after interacting, are absorbed back into their respective membranes.

Note that the multiplication of probabilities along a path shows the path probabilities, e.g., in the above, the specific evolution happens with probability $\frac{1}{2} \times \frac{1}{2} \times 1 = \frac{1}{4}$. We permit the probabilistic selection of a terminating process (0), which can reflexively transition to itself, and a membrane can terminate, transitioning to \emptyset , only if all processes inside a membrane are 0, as in line (4).

Quantum computation is essentially probabilistic and can be described by a classical Markov decision process. One such example is the repeat-until-success scheme, where the success of a quantum program component execution depends on the success observation of a measurement result. In the hidden subgroup algorithm for an additive group \mathbb{Z}_m , it is required to prepare a quantum superposition state $\frac{1}{\sqrt{m}} \sum_{j=0}^{m-1} |j\rangle$ (note: $m \leq 2^n$ might not be 2^n).

Example 3.5 (The State Preparation of Hidden Subgroup). We implement the distributed hidden subgroup algorithm as program $\{\{R\}\}_l, \{\{T'\}\}_r$, where the superposition preparation process as process R below². T teleports qubits from membrane l to r , and T' carries the rest of the computation of the hidden subgroup algorithm in membrane r .

$$R = \nu x(n). \nu y(1). x[0, n] \leftarrow \text{H}. x[0, n] \sqcup y[0] \leftarrow x < m @ y[0]. v \leftarrow \mathcal{M}^i(y[0]). \text{if } (v) R \text{ else } T$$

In executing the program, we might select membrane l to make a move to execute its process R . Locally, the execution of process R prepares the desired superposition state in a probability $\frac{m}{2^n}$. $x[0, n] \sqcup y[0] \leftarrow x < m @ y[0]$ is a quantum oracle operation to compare the basis-ket bitstrings (as natural numbers) in the quantum array x with the number m and store the result in $y[0]$. A simplified transition step is listed below, and the detailed transitions are given in Appendix D.3.

$$(\emptyset, \{\{R\}\}_l, \{\{T'\}\}_r) \longrightarrow \dots \xrightarrow{l.1.\frac{m}{2^n}} (\{\langle x[0, n] \rangle_l : \frac{1}{\sqrt{m}} \sum_{j=0}^{m-1} |j\rangle\}, \{\{T\}\}_l, \{\{T'\}\}_r)$$

²The $\nu x(n). R$ operation creates n qubit array x , with initial value $|\bar{0}\rangle$, used in the process R . This syntactic construct for constructing new arrays is presented in Appendix A.

We show the initial part of the MDP-based transition automaton for the program (Example 3.5) in Figure 3, as an evidence of showing the power of analyzing distributed quantum algorithms in MDP. Here, only the marked red part happens in the single process R above, and the top-level membrane execution is represented as the root node (marked back on the left) that has non-deterministic edges choosing l and r for execution. The $l.1$ edge points to the process-level execution in R and it represents that we choose to execute the process in l . The self-edge in the marked red node represents the $y[0]$'s measurement resulting in 0 with a probability $1 - \frac{m}{2^n}$, and the measurement of 1 moves to the next marked red node. Going through each edge results in a further probability reduction. For example, every step of measuring out 0 for $y[0]$ indicates going through the circular edge and results in a $1 - \frac{m}{2^n}$ probability reduction along the execution path from the root node to the current state.

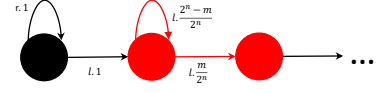


Fig. 3. Transition Automaton

3.3 Equivalence Relation for DisQ Programs

Given that DisQ program encodes distributed quantum programs, it is necessary to ensure the correctness of such encoding by comparing its behavior against the corresponding sequential quantum programs. Typically, the correctness is ensured by proving that any *relevant* behavior exhibited in the sequential program is also exhibited by its distributed counterpart, and vice versa. In process algebraic terms, such an equivalence is characterized using bisimulation, simulation, and trace equivalence relations. At a high level, these relations equate to the behavior of reachable configurations after one or more equivalent steps (see [Milner 1980] for details). Equivalence between steps is captured by the labels of the steps, and equivalence between configurations is decided by the valuations of variables that describe those configurations. In the context of distributed quantum programs (encoded by DisQ), such a notion of equivalence may not be appropriate.

First, the variables in the quantum programs involve both classical and quantum data. One of the key aspects of quantum data is that its impact is only manifested if measured. In other words, quantum states are not observable unless measured. Furthermore, the ordering of quantum operation on quantum data may not impact the result of its final measurement. For instance, applying an X gate followed by a Hadamard gate (H) on a qubit results in the same measure of the qubit when compared to the application of a H gate followed by a Z gate. However, simply comparing the measurement results might not capture the quantum natures that are not observable by sampling tests. For example, two quantum qubits have the states $\frac{1}{\sqrt{2}}(|0\rangle + |1\rangle)$ and $\frac{1}{\sqrt{2}}(|0\rangle - |1\rangle)$, i.e., the second state has a local phase. Clearly, the two quantum states are not equivalent, but sampling measurement results always produce a 50% chance of 0 or 1 for both states. On the other hand, quantum programs usually have ancillary qubits supporting the program execution, such as the $y[0]$ qubits in Example 3.5. The quantum states of these ancillary qubits do not affect the program's correctness. As a tradeoff, we make three adjustments in our equivalence relation: 1) we view quantum measurements on a locus as a sequence point for comparing the quantum states; 2) we provide labels i in the measurement syntax, as $x \leftarrow \mathcal{M}^i(\kappa)$, to indicate that the specific measurement operations should be ignored in the equivalence check; and 3) any quantum data not at the sequence point must not impact/decide the equivalence between the quantum configurations.

Second, the action labels in DisQ correspond to the location information capturing the nondeterministic choice and the probability associated with action for a process at the non-deterministically selected location. The specific location information, while important in describing programs in DisQ, is irrelevant for checking equivalence between two programs expressed in DisQ. A simple and

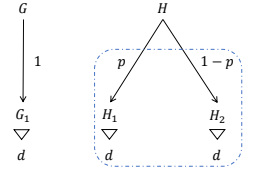


Fig. 4. Sim Diagram

Unitary Expr	μ
Bool Expr	B
Local Action	$A ::= \kappa \leftarrow \mu \mid x \leftarrow \mathcal{M}^{[i]}(\kappa)$
Communication Action	$D ::= a!v \mid a?(y)$
Process	$R, T ::= 0 \mid D.R \mid A.R \mid \text{if } (B) R \text{ else } T$
Membrane	$P, Q ::= \{\bar{R}\}_l \mid R\{\bar{T}\}_l \mid \partial c(n).P$

Fig. 5. DisQ Syntax. We have the syntactic sugar: $\text{if } (B) \{R\}.T = \text{if } (B) R.T \text{ else } T$. $[i]$ indicates the measurement result is ignored (having label i) or not. Other syntax is in Appendix A.

straightforward way to address this issue is to discard the location information when describing the equivalence relation. This leaves us with the problem of handling the probability information that labels each transition/step. This problem can be intuitively described as follows. Consider that there is a system that evolves from a configuration G with probability 1 to a configuration G_1 and consider another system that evolves from a configuration H with probability p to a configuration H_1 and with probability $1 - p$ to a configuration H_2 , shown in Figure 4. Assume that the configurations G and H have the same relevant data and measurements, and similarly, configurations G_1 and each of H_1 and H_2 have the same data and measurements d . By the standard notions of (bi)simulation equivalence, G will not be equivalent to H owing to the fact the probability of evolution to G to G_1 does not "match" with the probability of evolution from H to H_1 or H to H_2 . However, the probability measure for G to evolve to G_1 , and H to H_1 and H_2 are identical (i.e., 1).

Therefore, it is necessary to introduce a new notion of equivalence relation. At its core, this new equivalence relation is defined over the set of equivalent configurations. When a configuration evolves, we partition the destination configurations into equivalent classes, and we compute the probability of evolving to each equivalent class as the sum of the probabilities leading to each element in the class. For instance, in the above abstract example, G evolves G_1 with probability 1. On the other hand, H evolves to H_1 and H_2 , where H_1 and H_2 are identical and hence belong to the same equivalent class. The probability for evolving from H to the class containing H_1 and H_2 is $p + (1 - p) = 1$. Based on this observation, we can conclude that G is equivalent to H because they are identical, and each can evolve to equivalent classes G_1 and $\{H_1, H_2\}$ with probability 1.

We will elaborate and formalize this new notion of our equivalence relation in Section 5.

4 DisQ Formalism

This section presents the DisQ's syntax, semantics, type systems, and the type soundness theorem. We use distributed GHZ (Examples 3.2 and 3.3) as our running example.

4.1 Syntax for The DisQ Language

A DisQ encoding of a distributed quantum algorithm is described using a multiset of location-specific quantum processes. We define the syntax (Figure 5) over a membrane (a concept borrowed from the CHAM: see Section 3.1). There are three types of membrane descriptions: a multiset of processes ($\{\bar{R}\}_l$) with location information (l), an airlocked process associated with a membrane ($R\{\bar{T}\}_l$) and a membrane which evolves after a new length n channel ($\partial c(n)$) is initiated ($\partial x(n).P$). The last type is necessary to facilitate communication between processes in different membranes. The operation $\partial c(n)$ creates a quantum channel (c). If we have $\partial c(n).P, \partial c(n).Q$ with P and Q being in membranes l and r , they collaboratively create an $2n$ -qubit Bell pair, each membrane shares an n qubit array, pointed to by loci $\langle c[0, n] \rangle_l$ and $\langle c[0, n] \rangle_r$, respectively. This is similar to π -calculus style creation of new channels.

A process R , localized to a membrane, can be understood as a sequence of local (A) or communication actions (D). Here, we permit classical process algebraic message transmission operations ($a!v$ and $a?(y)$); they are the only communication actions that can perform direct message passing

between different membranes, and the manipulations of quantum channels are done through local quantum actions that might lead to global side effects. We include quantum unitary operation $\kappa \leftarrow \mu$, applying a unitary operation μ to a local locus κ , as well as quantum measurement $x \leftarrow \mathcal{M}^{[i]}(\kappa)$, measuring the qubits referred to by κ and storing the result as a bitstring x . In DISQ, we abstract away the detailed implementation of μ and assume that they can be analyzed by some systems describing quantum unitary circuits, e.g., VOQC [Hietala et al. 2023]. In a process, we also permit a classical conditional `if (B) R else T`. The expression B is arbitrary classical Boolean expression B , implemented using bit-arithmetic, i.e., 1 as true and 0 as false.

4.2 DISQ Semantics

The DISQ semantics is based on a combination of Markov-chain and Markov-decision process and can be divided into two categories, for process and membrane level semantics. The process level semantics is shown in Figure 6, which is expressed as a labeled transition system $(\varphi, R) \xrightarrow{\xi.p} (\varphi', T)$, where R and T are processes, φ and φ' are the pre- and post- local quantum states described in Figure 2, ξ is the transition label being empty (ϵ) or a quantum state, and p is the probability of the single step transition. The membrane level semantics defines the nondeterministic behaviors of a DISQ program, shown in Figure 7. It is formalized as a labeled transition system $(\Phi, \bar{P}) \xrightarrow{\alpha.p} (\Phi', \bar{Q})$ where α (either $l.\xi$ or $l.r.\xi$) captures the membrane locations (l or $l.r$) participating in the nondeterministic choice of the transition followed by a label (ξ), p represents the probability of the transition, and Φ and Φ' are the global pre- and post- quantum states described in Figure 2.

Process Level Semantics. A DISQ process is a sequence of actions, and rules in Figure 6 define the semantics for a local action prefixed in a process. Rule S-SELF shows that the process semantics in a membrane is reflexive and can make a move to itself to preserve the stochastic property in a Markov chain, explained shortly below. Rule S-OP applies a quantum unitary operation to a locus κ 's quantum data. Here, the locus fragment κ to which the operation is applied must be prefixed in the locus $\kappa \sqcup \kappa'$ that refers to the entire quantum data q . If not, we will first apply equivalence rewrites, explained in Section 4.3 and Li et al. [2024], to move κ to the front. With κ preceding the rest fragment κ' , the operation's semantic function $\llbracket \mu \rrbracket^n$ is then applied to κ 's position bases in the quantum value q . More specifically, the function is only applied to the first n (equal to $|\kappa|$) basis bits of each basis-ket in the value while leaving the rest unchanged. For example, in Example 3.3 line (4), to apply CX to the $\langle x[0, 2] \rangle_l$, we use rewrites to ensure that $x[0, 2]$ is prefixed in the locus and it is arranged as $x[0]$ followed by $x[1]$.

A measurement ($x \leftarrow \mathcal{M}^{[i]}(\kappa).R$) collapses qubits in a locus κ , binds a C-kind integer to x , and restricts its usage in R . Rule S-MEA shows the partial measurement behavior³. Assume that the locus is $\kappa \sqcup \kappa'$; the measurement is essentially a two-step array filter: (1) the basis-kets of the value is partitioned into two sets (separated by +): $(\sum_{j=0}^m z_j |d\rangle |d_j\rangle) + q\langle \kappa, d \neq \kappa \rangle$, by randomly picking a $|\kappa|$ -length basis d where every basis-ket in the first set have κ 's position basis d ; and (2) we create a new array value by removing all the basis-kets not having d as prefixes (the $q\langle \kappa, d \neq \kappa \rangle$ part) and also removing the κ 's position basis in every remaining basis-ket; thus, the quantum value becomes $\sum_{j=0}^m \frac{z_j}{\sqrt{p}} \eta_j$. Since the amplitudes of basis-kets must satisfy $\sum_i |z_i|^2 = 1$, we need to normalize the amplitude of each element in the post-state by multiplying a factor $\frac{1}{\sqrt{p}}$, with $r = \sum_{j=0}^m |z_j|^2$ as the sum of the amplitude squares appearing in the post-state. The rule's transition is labeled with $\xi.p$, referring to the quantum state before the measurement result, depending on having label i and the probability of having the result. An example i labeled measurement is Example 3.5, having

³A complete measurement is a special case of a partial measurement.

$$\begin{array}{l}
\text{S-SELF} \quad (\varphi, 0) \xrightarrow{1} (\varphi, 0) \\
\text{S-IFT} \quad (\varphi, \text{if } (1) R \text{ else } T) \xrightarrow{1} (\varphi, R) \\
\text{S-MEA} \quad p = \sum_j |z_j|^2 \quad \xi = \left(\sum_j z_j |d\rangle \eta_j + q(\kappa, d \neq \kappa) \right)^{2[i]} \\
\hline
(\varphi \cup \{\kappa \boxplus \kappa' : \sum_j z_j |d\rangle \eta_j + q(\kappa, d \neq \kappa)\}, x \leftarrow \mathcal{M}^{[i]}(\kappa).R) \xrightarrow{\xi.P} (\varphi \cup \{\kappa' : \sum_j \frac{z_j}{\sqrt{p}} \eta_j\}, R[d/x]) \\
\begin{array}{l}
\llbracket \mu \rrbracket^n (\sum_j z_j |d_j\rangle \eta_j) \triangleq \sum_j z_j (\llbracket \mu \rrbracket |d_j\rangle) \eta_j \quad \text{where } \forall j |d_j\rangle = n \\
(\sum_i z_i |c_i\rangle \eta_i + q) \langle \kappa, b \rangle \triangleq \sum_i z_i |c_i\rangle \eta_i \quad \text{where } \forall i. |c_i| = |\kappa| \wedge \llbracket b[c_i/\kappa] \rrbracket = \text{true}
\end{array}
\end{array}$$

Fig. 6. DisQ single process semantic rules. $q^{2[i]}$ results in q if i not show up, and ϵ otherwise.

$$\begin{array}{l}
\text{S-MEM} \quad \frac{n = |R, \bar{T}|}{(\Phi, \{D.R, \bar{T}\}_l) \xrightarrow{L, \frac{1}{n}} (\Phi, D.R\{\bar{T}\}_l)} \quad \text{S-MOVE} \quad \frac{n = |R, \bar{T}| \quad (\{\kappa : S^{|\kappa|}(q)\}, R) \xrightarrow{\xi.P} (\{\kappa' : q'\}, R')}{(\Phi \cup \{\langle \kappa \rangle_l \boxplus K : q\}, \{R, \bar{T}\}_l) \xrightarrow{L, \xi, \frac{p}{n}} (\Phi \cup \{\langle \kappa' \rangle_l \boxplus K : F(q')\}, \{R', \bar{T}\}_l)} \\
\text{S-COMM} \quad (\Phi, a!v.R\{\bar{M}\}_l, a?(x).T\{\bar{N}\}_r) \xrightarrow{L, r.1} (\Phi, \{R, \bar{M}\}_l, \{T[v/x], \bar{N}\}_r) \quad \text{S-REV} \quad (\Phi, R\{\bar{T}\}_l) \xrightarrow{L, 1} (\Phi, \{R, \bar{T}\}_l) \\
\text{S-NEWCHAN} \quad \frac{\text{loc}(P) = l \quad \text{loc}(Q) = r}{(\Phi, \partial c(n).P, \partial c(n).Q) \xrightarrow{L, r.1} (\Phi \cup \{\langle c[0, n] \rangle_l \boxplus \langle c[0, n] \rangle_r \mapsto \bigotimes_{j=0}^{n-1} (\sum_{d=0}^1 \frac{1}{\sqrt{2}} |d\rangle)\}, P, Q)} \quad \text{S-END} \quad (\Phi, \{\bar{0}\}_l) \xrightarrow{L, 1} (\Phi, \emptyset) \\
\begin{array}{l}
S^n (\sum_j z_j |c_j\rangle \beta_j (\beta'_j |l\rangle)) \triangleq \sum_j z_j \beta_j (|c_j\rangle \beta'_j |l\rangle) \quad \text{where } \forall j |c_j| = n \\
F(\sum_j z_j \beta_j (|c_j\rangle \beta'_j |l\rangle)) \triangleq \sum_j z_j |c_j\rangle \beta_j (\beta'_j |l\rangle)
\end{array}
\end{array}$$

Fig. 7. Membrane-level semantic rules. $\text{loc}(P)$ produces the location in membrane P .

transitions in Appendix D.3 step (5). Measurement operations cause locus scope changes in the quantum state, and DisQ ensures the program correctness by our type system in Section 4.3. Rule S-IFT and S-IFF describe the semantics of classical conditionals.

Membrane Level Semantics. Figure 7 shows the membrane level semantics. A DisQ program is a set of membranes. We assume that the evaluation of the membrane set is compositional, i.e., every subset of the set can make a move.

The transitions of the processes in a membrane can be understood as a Markov chain, in the sense that every process in a membrane has the chance to be selected to perform a location action or a communication action that requires an airlock step. This indicates that the chance of selecting any of the processes in a membrane equals $\frac{1}{n}$, where n is the number of processes in the membrane. The connection between a process transition and a membrane level transition, with the above probability chance calculation, is encoded as rules S-MEM and S-MOVE. The former handles the airlock mechanism for airlocking a process, ready for communication with another membrane, and the latter connects local action transitions with transition behaviors at the membrane level.

In S-MOVE, the locus $\langle \kappa \rangle_l \boxplus K$ is assumed to map to the data q in the quantum state, and the prefixed action in R coincidentally is applied to the locus κ (in membrane l), which is guaranteed by the DisQ type system. In evaluating one step action in R , we use the operator $S^{|\kappa|}$ to select the κ 's position bases and push the rest of the position bases to the frozen basis stacks. Once the process level transitions the state to $\kappa' : q'$, we pull back the frozen bases from the stacks through the operator F and manage the global final state for the global locus $\langle \kappa' \rangle_l \boxplus K$ to be $F(q')$. In the

$$\begin{array}{c}
\text{T-OP} \\
\frac{\Omega; \sigma \cup \{\kappa \boxplus \kappa' : \tau\} \vdash_l R \triangleright \sigma'}{\Omega; \sigma \cup \{\kappa \boxplus \kappa' : \tau\} \vdash_l \kappa \leftarrow \mu.R \triangleright \sigma'} \\
\\
\text{T-IF} \\
\frac{\Omega \vdash_l B : C \quad \Omega; \sigma \vdash_l R \triangleright \sigma' \quad \Omega; \varphi \vdash_l T \triangleright \sigma'}{\Omega; \sigma \vdash_l \text{if } (B) R \text{ else } T \triangleright \sigma'} \\
\\
\text{T-REV} \\
\frac{\Omega \vdash_l a : C \quad \Omega(l)[x \mapsto C]; \sigma \vdash_l R \triangleright \sigma'}{\Omega; \sigma \vdash_l a?(x).R \triangleright \sigma'} \\
\\
\text{T-NEWC} \\
\frac{\text{loc}(P) = l \quad \text{loc}(P') = r \quad \Omega(l)[c \mapsto Q(n)]; \Sigma_l \cup \{\langle c[0, n] \rangle_l : \text{EN}\} \vdash P \triangleright \Sigma'_l \quad \Omega(r)[c \mapsto Q(n)]; \Sigma_r \cup \{\langle c[0, n] \rangle_r : \text{EN}\} \vdash P' \triangleright \Sigma'_r \quad \Omega; \Sigma \vdash \bar{Q} \triangleright \Sigma'}{\Omega; \Sigma_l \cup \Sigma_r \cup \Sigma \vdash \partial c(n).P, \partial c(n).P', \bar{Q} \triangleright \Sigma'_l \cup \Sigma'_r \cup \Sigma'} \\
\\
\text{T-MEM} \\
\frac{\text{has_mea}(\bar{R}) \quad \neg \text{has_mea}(\bar{T}) \quad \forall j \in [0, |\bar{R}|). \Omega; \sigma_j \vdash_l \bar{R}_j \triangleright \sigma'_j \quad \Omega; \sigma \vdash_l \bar{T} \triangleright \sigma' \quad \Omega; \Sigma \vdash \bar{Q} \triangleright \Sigma'}{\Omega; \langle (\bigcup_{j \in [0, |\bar{R}|)} \sigma_j) \cup \sigma \rangle_l \cup \Sigma \vdash \{\{\bar{R}, \bar{T}\}_l, \bar{Q}\} \triangleright \langle (\bigcup_{j \in [0, |\bar{R}|)} \sigma'_j) \cup \sigma' \rangle_l \cup \Sigma'} \\
\langle \sigma \rangle_l \triangleq \forall \langle \kappa \rangle_r : \tau \in \langle \sigma \rangle_l . r = l
\end{array}$$

Fig. 8. DisQ type system. $\text{has_mea}(\bar{R})$ means every $R \in \bar{R}$ contains a measurement operation syntactically.

label $l.\xi.\frac{p}{n}$, we make a nondeterministic choice of location l , p is the probability of a one-step move in R , and ξ is the label associated with the location action transitions introduced in Figure 6. Rule S-REV permits the release of an airlock.

Note that, in DisQ, every membrane has a fixed amount of processes in its lifetime. In rules S-MEM and S-MOVE, each probabilistic choice of performing a process has a probability $\frac{1}{n}$ where n is the number of processes in the membrane. To guarantee the equal distribution of the probabilistic choice of a process, we include rule S-SELF in Figure 6, as a 0 process can make a move to itself. In the end, if every process in a membrane turns to 0, rule S-END permits its termination.

Rule S-NEWCHAN creates a new quantum channel between the membranes l and r , which results in a $2n$ -qubit Bell pair connecting l and r , each of which shares n qubits, referred to by the channel name c . The DisQ type system ensures that the two different c arrays are only used in the two different membranes, respectively; thus, no name collision is introduced. Rule S-COMM performs a classical message communication inherited from traditional π -calculus [Milner et al. 1992].

Both S-NEWCHAN and S-COMM transitions have labels $l.r.1$, meaning that the nondeterministic event happens across the l and r membranes. The probability 1 in the above three rules indicates that the transitions happen 100% once a nondeterministic choice is made.

4.3 DisQ Type System

The DisQ type system also has two levels of typing judgments. The membrane level judgment is $\Omega; \Sigma \vdash \bar{P} \triangleright \Sigma'$, stating that \bar{P} is well-typed under the environments Ω and Σ . The process level typing judgment is $\Omega; \sigma \vdash_l \bar{R} \triangleright \sigma'$, stating that \bar{R} is well-typed under the environments Ω and σ in membrane l . The C-mode variables in a kind environment Ω are populated through message receipt and quantum measurement operations, while the Q-kind variables are populated through a channel $\partial c(n)$ creation operation. The type rules are in Figure 8. For every type rule, well-formed domains ($\Omega \vdash \text{dom}(\Sigma)$) (or $(\Omega \vdash_l \text{dom}(\sigma))$) are required but hidden from the rules, such that every variable used in all loci of Σ (or σ) must appear in Ω . The type system enforces three properties below.

Ensuring Proper Parameter Kinds and Scopes. The type system ensures the scoping properties in variables and channels, e.g., quantum channels and variables have kind $Q(n)$, while classical channels and variables have kind C . Quantum variables and channels can possibly be modified inside a membrane but cannot be referred to by operations from distinct membranes, and some operations, such as message sending and receiving, can only refer to classical variables and channels. All these

scoping properties are enforced by the type system. The Boolean ($\Omega \vdash_l B : C$) and arithmetic ($\Omega \vdash_l v : C$) expression checks (Appendix B) in rules T-IF, T-SEND, and T-REV, ensure that these expressions can only produce classical results and that their parameters are classical.

Ensuring Proper Locus Partitioning and Locality. The type system also ensures that loci are properly partitioned in different membranes, and each membrane refers only to the permitted local loci. Rules T-MEM and T-NEWC partition loci by partitioning type environment, indicated by \cup , into pieces for different membranes. Rule T-MEM ensures a properly separated analysis of different loci and quantum parameters in different membranes, where the structure $\langle \sigma \rangle_l$ is a subset of the type environment and represents a procedure of collecting all the loci referred to membrane P residing in location l , and type check P with the subset $\langle \sigma \rangle_l$. T-NEWC enables the individual analysis of quantum channels shared by the two membranes, e.g., the quantum channel referred to by the locus $\langle c[0] \rangle_l \sqcup \langle c[0] \rangle_r$, in Example 3.2. In analyzing the channel creation, we separately have a type environment Σ_l with $\langle c[0] \rangle_l : \text{EN}$ to type check P , and another type environment to type check P' .

Specifically, we ensure that the measurement locus scopes properly partitioned and preserved. For example, rule T-IF requires the output type environments to be the same for the two branches (σ'). This indicates that if one branch contains a measurement on certain loci, the other branch must contain a similar measurement of these loci. In rule T-MEM, depending on whether or not a process contains measurement operations (has_mea), the quantum qubit resource sharing scheme is different. We collect all the local loci ($\bigcup_{j \in [0, |\bar{R}|)} \sigma_j$) $\cup \sigma$ in l , and partition the set further into different disjoint union sets. For the processes \bar{R} , containing measurement operations, we type check each R with a disjoint set σ_j . This forbids R the possibility of sharing qubits with other processes. If a process contains a measurement, it is not suitable for having single-location concurrent behaviors with other processes because this would create the potential that other processes might refer to a measured qubit. For the processes \bar{T} , having no measurements, we permit a shared qubit set σ .

Guiding Locus Equivalence and Rewriting. The DisQ type system maintains the simultaneity of loci in type environments and quantum states through the type-guided state rewrites, formalized as equivalence relations. We saw the GHZ examples in Example 3.3 that we might need to merge two entanglement groups or rearrange the qubit positions in loci. Such rewrites are formulated as type equivalence relations, which are associated with simultaneous quantum state rewrites; the details are introduced in Li et al. [2024] and Appendix A. Here, we provide a taste of how such rewrites can happen. A locus represents a possibly entangled qubit group. In many cases, we need to utilize the locus information in the type environment to guide the equivalence rewrites of states guarded by the locus. We associate a state φ , with a type environment σ by sharing the same domain, i.e., $\text{dom}(\varphi) = \text{dom}(\sigma)$. Thus, the environment rewrites (\leq) happening in σ gear the state rewrites (\equiv) in φ . One example rewrite is to add an additional qubit $x[j+1]$ to a local locus $x[0, j]$, and rewrite it to $\kappa(x[j-1] \sqcup x[0, j-1] \sqcup x[j])$, which can also cause the state rewrites happen accordingly as (from left to right):

$$\begin{aligned} \{x[0, j] : \text{EN}\} \cup \{x[j] : \text{EN}\} &\leq \{x[0, j+1] : \text{EN}\} &&\leq \{\kappa : \text{EN}\} \\ \{x[0, j] : \Sigma_{d=0}^1 \frac{1}{\sqrt{2}} |\bar{d}\rangle |1\rangle\} \cup \{x[j] : |0\rangle\} &\equiv \{x[0, j+1] : \Sigma_{d=0}^1 \frac{1}{\sqrt{2}} |\bar{d}\rangle |1\rangle |0\rangle\} &\equiv \{\kappa : \Sigma_{d=0}^1 \frac{1}{\sqrt{2}} |1\rangle |\bar{d}\rangle |0\rangle\} \end{aligned}$$

The DisQ Metatheory. We prove our type system's soundness with respect to the semantics, assuming well-formedness. The type soundness theorem is split into type progress and preservation. The theorems rely on the definitions of wellformed domains ($\Omega \vdash \Sigma$) and wellformed states ($\Omega; \Sigma \vdash \Phi$), shown in Appendix C. The progress theorem shows that a well-typed DisQ program can always make a move without resulting in deadlocks. Certainly, a DisQ program can diverge, leading to future studies.

THEOREM 4.1 (TYPE PROGRESS). If $\Omega \vdash \Sigma$, and $\Omega; \Sigma \vdash \Phi$, there exists α, Σ' and \bar{P}' , $(\Phi, \bar{P}) \xrightarrow{\alpha} (\Phi', \bar{P}')$.

Type preservation states that our type system ensures the three properties above and that the DisQ semantics can describe all different quantum operations without losing generality because we can always use the equivalence rewrites to rewrite the locus state in ideal forms.

THEOREM 4.2 (TYPE PRESERVATION). If $\Omega \vdash \Sigma$, $\Omega; \Sigma \vdash \bar{P} \triangleright \Sigma'$, $(\Phi, \bar{P}) \xrightarrow{\alpha} (\Phi', \bar{P}')$, and $\Omega; \Sigma \vdash \Phi$, then there exists Ω_1 and Σ_1 , $\Omega_1; \Sigma_1 \vdash \bar{P}' \triangleright \Sigma'$.

5 DisQ Observable Simulation

Here, we formally define the DisQ simulation, where we are interested in universal path properties, e.g., for all computation paths, the probability of a specific measure result is p ; such properties enable the construction of equivalence between a quantum program and its distributed version.

To utilize DisQ to rewrite a sequential quantum program to a distributed one, it is necessary to develop an equivalence checker to show the two programs are semantically equivalent; such a task is typically tackled through (bi)simulation, i.e., two programs are equivalent, if and only if they are (bi)similar. As in Section 3.3, the traditional (bi)simulation might be too strong to show the equivalence between a sequential and a distributed program. We define the DisQ observable simulation relation based on the marking sequence points of measurement operations without labels i , the core component of the DisQ equivalence checker; example utilities are in Section 6.

The DisQ semantics (Section 4) describe a labeled transition system $(\Phi, \bar{P}) \xrightarrow{\alpha.p} (\Phi', \bar{P}')$, where Φ and Φ' are quantum states, \bar{P} and \bar{P}' are DisQ programs, and $\alpha.p$ is a label; α is either a label in the DisQ semantics ($l.\xi$ or $l.r.\xi$), or an invisible label (ϵ). We can view a pair (Φ, \bar{P}) of quantum state and DisQ program as a transition configuration. The DisQ observable simulation is defined over finite sets of configurations, named as G or H , each element in the set has the form $(\Phi, \bar{P})^p$, where (Φ, \bar{P}) is a transition configuration and the probability p is the accumulated probability. We define a syntactic sugar G^p (or H^t), where the extra flag p (or t) refers to that for all $(\Phi_j, \bar{P}_j)^{p_j}$, $p = \sum_j p_j$ (or $t = \sum_j p_j$), with $j \in [0, |M|)$. We also allow users to define label mask functions $\psi: \alpha \rightarrow \alpha$ to mask a specific set of labels to be invisible, i.e., users are allowed to perform $\psi(\alpha.p) = \alpha.p$ or $\psi(\alpha.p) = \delta.p$, where $\delta = \xi$ or $\delta = \epsilon$. We first define set transitions related set of transition configurations G below.

Definition 5.1 (DisQ Configuration Set Transition). Given a transition configuration set G , we define set transition $G \xrightarrow{\alpha} G_1^t$ below.

- for every $(\Phi_j, \bar{P}_j)^{p_j}$ in G , we have $(\Phi_j, \bar{P}_j) \xrightarrow{\alpha.t_j} (\Phi'_j, \bar{P}'_j)$, and G_1 contains all configurations $(\Phi'_j, \bar{P}'_j)^{p_j * t_j}$ transitioned from (Φ_j, \bar{P}_j) , and $t = \sum_j p_j * t_j$, with $j \in [0, |G|)$.

Definition 5.2 (DisQ Observable Simulation). Given two transition configuration sets G and H , G simulates H , written as $G \sqsubseteq H$, iff

- $G = G_1 \cup G_2$, $G_1 \xrightarrow{\alpha} G_3^p$, where $\alpha \neq \epsilon$, if there is H_1, H_2, H_3 , such that $H = H_1 \cup H_2$, and $H_1 \xrightarrow{\alpha} H_3^t$, and $p \approx t$, and $G_3 \cup G_2 \sqsubseteq H_3 \cup H_2$.
- $(\Phi, \bar{P}) \xrightarrow{\epsilon.p'} (\Phi', \bar{P}')$ with $(\Phi, \bar{P})^p \in G$, then $(G - \{(\Phi, \bar{P})^p\}) \cup \{(\Phi', \bar{P}')^{p * p'}\} \sqsubseteq H$.
- $(\Phi, \bar{Q}) \xrightarrow{\epsilon.t'} (\Phi', \bar{Q}')$ with $(\Phi, \bar{Q})^t \in H$, then $G \sqsubseteq (H - \{(\Phi, \bar{Q})^t\}) \cup \{(\Phi', \bar{Q}')^{t * t'}\}$.

One can develop a (on-the-fly) algorithm for observable simulation as a least fixed point computation of negation of simulation relation [Basu et al. 2001]. Instead of computing $G \sqsubseteq H$, we compute $\text{not_sim}(\{G\}, \{H\}) \triangleq \neg(G \sqsubseteq H)$. Here, we start with two configuration sets, each containing only the initial configurations, i.e., \bar{G} and \bar{H} are respectively initialized as $\{G\}$ and $\{H\}$, as they contain all the possible initial states for the two programs being simulated. In each iteration, we partition a

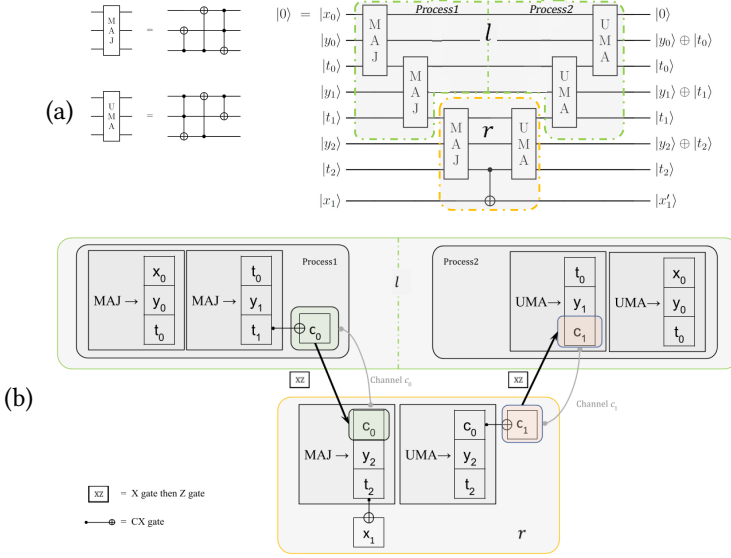


Fig. 9. Ripple-Carry adder circuits. (a): sequential version, (b): distributed version. x'_1 is the overflow bit.

configuration set in the different sets, if the transition configuration set leads to different labels, e.g., in the first iteration, we partition \bar{G} into different sets, such as $G = G_1 \uplus G_2 \uplus \dots$, for each G_j , we guarantee that $G_j \xrightarrow{\alpha_j} G_j^p$ for one observable label α_j . Then, we check if there is also a partition in H , such that $H = H_1 \uplus H_2 \uplus \dots$, for each H_j , we make sure that $H_j \xrightarrow{\alpha'_j} N_j^u$ for the same label α'_j . For G_j , if we cannot find H_j , such that $G_j \sqsubseteq H_j$, the `not_sim` predicate holds. Otherwise, we loops to check `not_sim` ($\{G_j\}, \{H_j\}$). We take the least-fixed point of the computation, and the negation of the computation result conducts the simulation relation between G and H .

We implement a DisQ interpreter in Java and implement the `not_sim` function on top of our DisQ interpreter as our simulation checker. We then utilize the simulation checker to validate the simulation relation between sequential quantum programs P and their distributed versions \bar{P} , i.e., $\bar{P} \sqsubseteq P$. Since P is typically a sequential program, a simulation check is enough to equate the two. Certainly, one can easily construct a bisimulation checker based on our simulation framework for other utilities. We enable the simulation checks for all case studies in the paper.

6 Case Studies

We show two examples of utilizing distributed systems to develop quantum distributed algorithms, with more in Appendix D. We show a small cost evaluation, based on the DisQ modeling for distributed quantum channels, in Section 6.3.

6.1 Distributed Quantum Adders

Quantum oracle circuits are reversible and used as subroutines in many quantum algorithms; they usually perform the quantum version of some classical computations, e.g., the oracle component in Shor's algorithm is a quantum version of a modulo-multiplication circuit. They are usually the most resource-consuming component in a quantum circuit [Li et al. 2022] and can be implemented as arithmetic operations based on quantum addition circuits. Distributing the execution of oracle circuits to remote machines can greatly mitigate the entanglement resource needs in a single location. Here, we show the example of distributing a quantum ripple-carry adder [Cuccaro et al. 2004]. We also describe the distributing QFT-based adders in Appendix D.2.

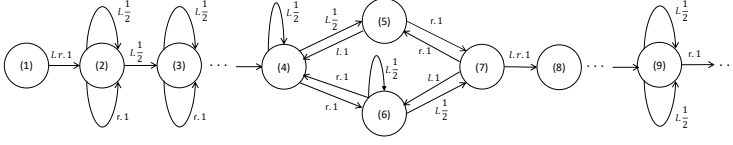


Fig. 10. The adder automaton.

Figure 9a shows the sequential circuit of a three-qubit ripple-carry adder, where we add the value of a three-qubit array t to the value stored in the three-qubit array y , with a two-qubit array x storing extra carry qubits, one for the initial carry and the other for an overflow indicator.

$$x[0] \sqcup y[0] \sqcup t[0] \leftarrow \text{MAJ}. x[0] \sqcup y[0] \sqcup t[0] \leftarrow \text{UMA}. 0$$

A quantum ripple-carry adder is constructed by a series of MAJ operations followed by a series of UMA operations, each of which has a diagram on the left side of Figure 9a. To understand the effect of the MAJ and UMA pairs, we show the application of such a pair to qubits $x[0]$, $y[0]$, and $t[0]$ above. Here, $x[0]$ is a carry flag for lease significant bits, and $y[0]$ and $t[0]$ are the two bits to add. The application of the MAJ operation adds $t[0]$ to $y[0]$, computes the carry flag for the next significant position, and stores the bit in $t[0]$. The application of the UMA operation reverses the computation in $x[0]$ and $t[0]$ back to their initial bits, but computes the additional result of adding $x[0]$, $y[0]$, and $t[0]$, stored in $y[0]$. As shown in Figure 9a, we arrange the MAJ and UMA sequences in the pattern that every MAJ and UMA pair is placed to connect a carry bit and two bits in the same significant position of arrays y and t . The CX gate in the middle of the circuit produces the overflow flag stored in $x[1]$. We define these steps in DISQ as the following operations.

We distribute the adder to be executed in two membranes, l and r , as shown in Figure 9b. Here, we further concurrently execute the two MAJs and UMAs, respectively, through two different processes in l . To enable the communication between l and r , we utilize the two processes, Te and Rt in Example 3.1 for performing membrane-level quantum data transmission based on quantum teleportation. Below, we define the distributed ripple-carry adder (Figure 9b).

Example 6.1 (Distributed Ripple-Carry Adder). The following program represents a 3-qubit distributed ripple-carry addition circuit and has two membranes l and r . Qubits $x[0]$, $y[0, 2]$, and $t[0, 2]$ belong to membrane l , and qubits $x[1]$, $y[2]$, and $t[2]$ belong to membrane r . Qubit arrays y and t are the input qubits storing two 3-qubit bitstrings as numbers, y stores the final output of adding the two numbers, and $x[0]$ is an ancilla initial carry qubit, $x[1]$ stores the overflow bit.

$$\begin{aligned} \partial c(2). \{ & \{x[0] \sqcup y[0] \sqcup t[0] \leftarrow \text{MAJ}. t[0] \sqcup y[1] \sqcup t[1] \leftarrow \text{MAJ}. Te(u[1], c[0]). 0, \\ & Rt(c[1]). t[0] \sqcup y[1] \sqcup c[1] \leftarrow \text{UMA}. x[0] \sqcup y[0] \sqcup t[0] \leftarrow \text{UMA}. 0\}_l, \\ \partial c(2). \{ & \{Rt(c[0]). c[0] \sqcup y[2] \sqcup t[2] \leftarrow \text{MAJ}. t[2] \sqcup x[1] \leftarrow \text{CX}. c[0] \sqcup y[2] \sqcup t[2] \leftarrow \text{UMA}. Te(c[0], c[1]). 0\}_r \end{aligned}$$

In this program, membranes l and r represent different quantum computers. We assume each permits an entanglement of maximal 6 qubits, which means that each computer is not enough to execute the three-qubit adder, requiring 8 qubits for execution, so they need to collaborate in executing the adder. We utilize the first process in membrane l to compute the two MAJ applications to y and t , then teleport $t[1]$ to membrane r to compute the addition of the third qubits ($y[2]$ and $t[2]$). The teleportation relies on the quantum channel $\langle c[0] \rangle_l \sqcup \langle c[0] \rangle_r$ and stores $t[1]$'s information in $\langle c[0] \rangle_r$. Membrane r deals with the third qubits with $t[1]$'s information in $\langle c[0] \rangle_r$ and teleports the result carry bit $c[0]$ to the second process in membrane l , via the quantum channel $\langle c[1] \rangle_l \sqcup \langle c[1] \rangle_r$; the $c[0]$ bit is stored in $\langle c[1] \rangle_l$. The second process in membrane r applies the remaining UMA operations. In the procedure of teleporting qubit $t[1]$ to $c[0]$ in membrane r , as well as teleporting qubit $c[0]$ in membrane r to $c[1]$ in membrane l , the $t[1]$ and $c[0]$ qubits are destroyed, so the total number of entangled qubits in every given time of a membrane is less than 6.

To show the equivalence between the sequential ripple-carry adder and its distributed version, we have the following proposition. Since the DisQ simulation requires sequence points of measurements, we assume that the sequential adder and its distributed version are extended with measurement operations at the end to measure all qubits.

PROPOSITION 6.2 (DISTRIBUTED ADDITION SIMULATION). Let Dis-Adder refer to the distributed ripple-carry adder program in Figure 9b and Adder refer to the sequential ripple-carry adder algorithm in Figure 9a, if we equate t_1 in Adder and c_1 in Dis-Adder, thus, $\text{Dis-Adder} \sqsubseteq \text{Adder}$.

To understand the simulation in Proposition 6.2, we need to understand the probabilistic transitions in the distributed adder, shown as an automaton in Figure 10. The (1) step creates a two-qubit quantum channel in membranes l and r . The label $l.r.1$ means that we make a non-deterministic choice in l and r with a probability 1, referring to only one way of making the channel creation. The (2) transition step has three possibilities. The transitions in the second process in l (having a label $l.\frac{1}{2}$) and membrane r (having a label $r.1$) represent airlocks on membranes l and r , respectively, but the airlocks are message receiving operations that are not available at this point; thus, the next very next steps of the two transitions can only perform releasing the airlocks through S-REV. This is why two self-edges point to (2) in Figure 10. The only transition, pushing step (2) to step (3) in the automaton, is the execution of the first process in membrane l (Figure 9b) to execute an MAJ operation. The label $l.\frac{1}{2}$ means that the transition is one of two possible choices in membrane l . The same situation happens in step (3), as an MAJ operation in the first process in l can push the automaton towards the next step.

Steps (4) to (8) in the automaton represent the procedure that passes a classical message from membrane l to r . In step (4), l 's second process is still waiting to receive a message, but l 's first process and membrane r can perform two airlocks, representing a classical communication can be established between the two. Depending on which of the two airlocks performs first, we can transition to either (5) or (6) for performing one of the airlocks, followed by edges from (5) and (6) to (7), indicating the other airlock transition. Since airlocks can be released, we have backward edges from (7) to (5) and (6) and edges from (5) and (6) to (4). The transitions from (7) to (8) commit the message-passing communication between membranes l and r . Transition (9) performs a local action in membrane r . At this point, the prefixed actions in the two processes in membrane l do not change program states, i.e., the first process in l is 0, possibly performing S-SELF, and the second process is waiting to receive a classical message from membrane r . Therefore, we have two self-edges in (9) labeled with l .

The simulation of the sequential and distributed adders' program transitions equates to two sets of program states reaching the same states before measurements. In our Java simulation checker, we implement the `not_sim` algorithm in Section 5. In each node in the transition automata, e.g., Figure 10, we collect the set of nodes for the next possible moves, with the validation of equating the label values on the two sides of the simulation. Quantum data are represented as symbolic values in our checker, and we validate the equivalence of two quantum data by performing property-based testing with many randomly generated assignments for the symbolic values to check the validity of the logical equivalences of quantum data predicate representations.

6.2 Distributed Shor's Algorithm

Shor's algorithm [Shor 1994], a well-known quantum algorithm potentially showing quantum advantages, factorizes a large number, and its core part is the quantum order finding circuit. Unfortunately, the quantum computing power required to execute Shor's algorithm, particularly in terms of the number of qubits, currently exceeds our available capabilities. Some studies [Xiao et al. 2023; Yan et al. 2022; Yimsiriwattana and Lomonaco Jr. 2004] are exploring more effective algorithm

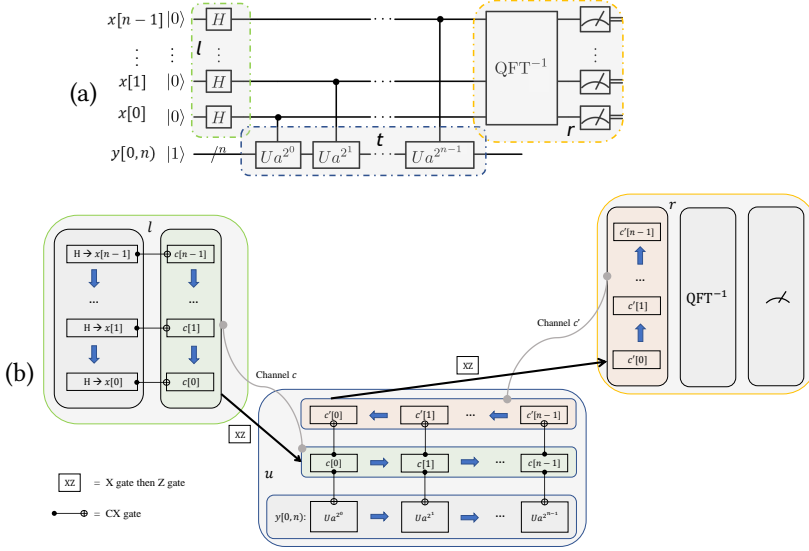


Fig. 11. The quantum order finding circuit of Shor's algorithm. (a): sequential version, (b): distributed version. execution methods. Notably, several of these works highlight the potential of rewriting Shor's algorithm in a distributed manner to reduce the number of entangled qubits needed on a single machine. There are two main observations regarding these algorithms: first, they aim to distribute the quantum component involved in order-finding; second, they utilize quantum teleportation to delegate parts of the order-finding process to different machines for execution. These studies illustrate one or two specific cases of how the algorithm can be effectively distributed.

Here, we show a way of distributing Shor's algorithm through DisQ and show the simulation between the sequential (Figure 11a) and the distributed versions (Figure 11b). Given two n -length qubit arrays $x[0, n]$ and $y[0, n]$, the order finding part (Figure 11a) of Shor's algorithm can be divided into three components: 1) we apply n Hadamard gates H to prepare the superposition state in $x[0, n]$, 2) we use an n step for-loop to apply a controlled- U operation, controlling on $x[j]$ and applying U to $y[0, n]$ for $j \in [0, n)$, each $U(v^{2^j})$ operation applies a modulo-multiplication $v^{2^j} * y[0, n] \% N$ to the qubit array $y[0, n]$, and 3) we apply QFT^{-1} and measurement, as the phase estimation step, to $x[0, n]$. We now show the distributed version below.

Example 6.3 (Distributed Shor's Algorithm). We show below a distributed quantum order finding algorithm, the quantum component of Shor's algorithm, using three membranes l , u , and r . Initially, l and u holds n -qubit x and y qubit arrays, respectively, while membrane r does not hold any qubits. $x[0, n]$ has initial state $|0\rangle$, while $y[0, n]$ qubit array has initial state $|1\rangle$. Membranes l and u share an n -qubit quantum channel c , while membranes u and r share an n -qubit quantum channel c' .

Processes:

$$\begin{aligned}
 He(j) &= x[j] \leftarrow H.Te(x[j], c[j]) & HeR(n) &= Rec(0, n, He) \\
 Me(j) &= Rt(c[j]) \cdot c[j] \boxtimes y[0, n] \leftarrow CU(v^{2^j}, N) \cdot Te(c[j], c'[j]) & MeR(n) &= Rec(0, n, Me) \\
 Ed(j) &= Rt(c'[j]) & EdR(n) &= Rec(0, n, Ed)
 \end{aligned}$$

Membranes:

$$\partial c(n) \cdot \{HeR(n)\}_l, \partial c(n) \cdot \partial c'(n) \cdot \{MeR(n)\}_u, \partial c'(n) \cdot \{EdR(n) \cdot c'[0, n] \leftarrow QFT^{-1} \cdot w \leftarrow \mathcal{M}(c'[0, n]) \cdot ps(w)\}_r$$

The above distributed Shor's algorithm is shown as the circuit diagram in Figure 11b. The purpose of the distribution is to put x and y qubit arrays in two different machines, so the entangled qubit numbers are limited to $n + 1$ in each machine. To do so, we create three different membranes l , u , and r to handle the three tasks in the order finding part above. Membrane l is responsible to

prepare superposition qubits in x array through the *HeR* process; we apply a H gate to $\langle x[j] \rangle_l$ and CX gate to the $\langle x[j] \rangle_l$ and $\langle c[j] \rangle_l$ qubits. Membrane u entangles x and y arrays by executing the for-loop through the *MeR* process; we apply n controlled- U gates between $\langle c[j] \rangle_u$ and the y array to entangle these two and apply n CX gates between the $\langle c[j] \rangle_u$ and $\langle c'[j] \rangle_u$ qubits. Membrane r applies the phase estimation step on the x array through the *EdR* process; it applies QFT^{-1} and measurement to locus $\langle c'[0, n] \rangle_r$ once $c'[0, n]$ qubits are received.

We now explain the communications among the three membranes. Assuming that two n -length quantum channels c and c' are created, the communications among the three membranes are managed by c and c' , indicated by the channel edges in Figure 11b, and they are managed in an n -step loop structure. In each j -th loop step, we use one qubit Bell pair in the quantum channel c , connecting l and u as $\langle c[j] \rangle_l$ and $\langle c[j] \rangle_u$, to transform the information in $x[j]$ in membrane l to $\langle c[j] \rangle_u$ in membrane u ; such a procedure is finished by single qubit teleportation. The j -th loop step also contains several operations in membrane u . Here, we first apply the controlled- U and CX gates mentioned above, and then perform a single qubit teleportation to transform the information in $\langle c[j] \rangle_u$ to $\langle c'[j] \rangle_r$ in membrane r . The blue arrow in Figure 11b indicates the order of each loop step, including a single qubit teleportation for transforming $\langle x[j] \rangle_l$ to $\langle c[j] \rangle_u$ and another teleportation for transforming $\langle c[j] \rangle_u$ to $\langle c'[j] \rangle_r$. After the communication loop is executed, we then apply the QFT^{-1} and measurement in membrane r to $\langle c'[0, n] \rangle_r$ at once. The application $ps(w)$ in Example 6.3 refers to the post-processing step after the quantum order funding step.

In every loop step, membrane u only holds $n + 1$ qubits; once the qubit $\langle c[j] \rangle_u$ is destroyed after its information is transferred to membrane r . This discussion omits the fact that the modulo multiplication circuit in membrane u might require many more ancillary qubits, which can be handled based on future circuit distribution, such as the addition circuit distributions in Section 6.1. To equate Shor's algorithm with the distributed version, we have the following proposition. It is trivial to see that the distributed version simulates the original Shor's algorithm since each membrane above contains only one process, i.e., there is no concurrency, and non-determinism is synchronized by classical message passing.

PROPOSITION 6.4 (DISTRIBUTED SHOR'S ALGORITHM SIMULATION). Let Dis-Shors refer to the distributed Shor's program in Figure 11b and Shors refer to the sequential one in Figure 11a, with two n -length input qubit arrays x and y ; if we equate the qubit array x in Shors and the qubit array c' in membrane r in Dis-Shors, thus, $\text{Dis-Shors} \sqsubseteq \text{Shors}$.

We utilize the same `not_sim` simulation checking procedure in Section 6.1 to validate Proposition 6.4.

6.3 Cost Evaluation Framework and Data Evaluation

	RC-adder	Shor's	GHZ
# Membranes	2	3	2
Max # of Qubits per Memb	7	$n+1$	n
# Gates + Overhead Gates	$19 + 120$	$\sim 424n^3 + 1954n^2 + 60n$	$2n + 60$

Table 1. Comparison of quantum circuits for different algorithms

It is important to use DisQ not only for distributing quantum algorithms but also for evaluating the cost of such distributions. In the DisQ formalism, as we demonstrate, the separation between regular quantum operations within processes and quantum channels for cross-boundary quantum communication facilitates this evaluation. As shown in Table 1, the marked red numbers are the overhead estimations of distributed algorithms (GHZ and the two algorithms above). We count the gate numbers in a circuit as the execution time estimation. The overhead estimation is based on

the ratio between the execution time of standard gates and quantum networking devices in real-world experimental data [Chu et al. 2024], where communication via a remote location quantum teleportation is about 60 times slower than a standard quantum gate (1 or 1 qubit gate).

From the table, we can see that the overhead cost of distributing algorithms will become lower if we deal with more comprehensive quantum algorithms, e.g., in the simple quantum adder example, the overhead is large, but the overhead of distributing Shor’s algorithm can be neglected. In GHZ, the distributing cost is manageable if n is greater than 100, which is a typical size in real-world applications [Mandelbaum et al. 2023].

The second row of the table shows the number of needed coherent qubits in each membrane, a.k.a. each single-location quantum computer. We only need a constant number of membranes to reduce the qubit number in a membrane. In general, if we want to deal with a very large quantum circuit, such as using Shor’s algorithm to factorize a number with $n = 2,000$ bits, we might need \sqrt{n} different membranes to maintain the maximum number of qubits in each membrane to be \sqrt{n} . In this scenario, the overhead of Shor’s algorithm is $60n^{\frac{3}{2}}$, which is still a tiny number compared to the algorithm’s circuit size.

7 Related Work

Many previous studies inspire the DisQ development.

Concurrent Quantum Frameworks. Many previous works studied the possibilities of quantum concurrency, in which a quantum program can be partitioned and run in a multi-threaded environment. Ying and Feng [2009] proposed an algebraic logical system to help partition a sequential quantum program into sub-components that can be executed in parallel, blurring providing the properties on how a distributed quantum system can be constructed. Partitioned components might share qubits, which indicates that the proposed partitions represent a concurrent system. Feng et al. [2022] proposes a proof system for concurrent quantum programs based on quantum Hoare logic [Ying 2012]. Ying et al. [2018, 2022] carefully design a quantum concurrent proof system by combining the above two works to permit the concurrent quantum program verification. Zhang and Ying [2024] extended the quantum concurrent proof system with the consideration of atomicity.

Eisert et al. [2000] showed theoretically the resource estimation of implementation a non-local gate, without investigating the forms how long-distance entanglement can be established. Ardeshir-Larijani et al. [2014] developed equivalence checkers for concurrent quantum programs, while Ardeshir-Larijani et al. [2013] developed an equivalence checker for quantum networking protocols.

These works primarily focus on reasoning about quantum concurrent behaviors, assuming the existence of distributed quantum programs and viewing the interactions among various distributed components as concurrent processes. In contrast, DisQ identifies methods for constructing distributed quantum systems and analyzes how a sequential program can be transformed into a distributed one, along with the implications of such distribution. The proof systems proposed by Ying et al. [2018, 2022] assume that communication occurs through classical channels (unlike in our case, where we also consider quantum teleportations as a means for communication). Additionally, Zhang and Ying [2024] address atomicity, exploring the consequences when two concurrent quantum programs manipulate the same qubits.

Quantum Process Algebra. Tafiiovich and Hehner [2009] proposed a framework to specify quantum network protocols. The DisQ’s design was inspired by several existing quantum process calculi: qCCS [Feng et al. 2012; Qin et al. 2020; Ying et al. 2009], Communicating Quantum Processes (CQP) [Gay and Nagarajan 2005], quantum model checker (MQC) [Davidson et al. 2012; Gay et al. 2013], QPAlg [Jorrand and Lalire 2004], and eQPAlg [Haider and Kazmi 2020]. These process calculi are developed to describe quantum networking and security protocols.

These quantum process calculi focus on modeling the concurrent aspects of quantum network protocols through classical message-passing models. Qubits or references to qubits are passed via different local parties (membranes). In DisQ, we model the distributed quantum environment, where qubits are local to a membrane, and the communications need special quantum channels to conduct. In addition, the DisQ semantics is based on Markov decision processes with probabilistic features, which are utilized in our set simulation relation based on classical Markov decision processes to check the equivalence between sequential and distributed quantum programs. This semantic design allows us to use existing works on classical probability verification to reason about the probabilities of quantum measurements. In contrast, previous works only capture the non-determinism in their semantic designs, and their quantum simulation relations are based on building a simulation relation over density matrices as quantum states.

Traditional Process Algebra. Communicating Sequential Processes (CSP) [Hoare 1985] and Π -calculus [Milner et al. 1992] are process calculi suitable for defining concurrent systems based on the message-passing model. Several bisimulation and trace-refinement protocol verification methodologies exist for CSP and the Π -calculus [Gibson-Robinson et al. 2014; Ltd. 2010; Sangiorgi 1993]. The Chemical Abstract Machine [Berry and Boudol 1992] is the inspiration of DisQ.

Quantum Network Protocols and Some Early Distributed Works. Building quantum internet and distributed systems was a long-existing dream for many researchers, with many theoretical and implementation works. For example, [Beals et al. 2013] showed a theory of performing distributed quantum via quantum random access memory. Below, we mainly focus on works showing implementability via NISQ computers. Quantum teleportation [Bennett et al. 1993; Rigolin 2005] serves as the basis for quantum communication between two parties. Julia-Diaz et al. [Juliá-Díaz et al. 2005] provides a two-qubit quantum teleportation protocol. Superdense coding [Bennett and Wiesner 1992] encodes a classical message into a quantum channel. Quantum routing investigates long-distance quantum message transmission, with quantum entanglement swaps being one of the promising protocols for the task [Kozłowski et al. 2020; Pirandola et al. 2017; Wehner et al. 2018]. QPass and QCast are protocols based on the quantum-swap algorithm [Shi and Qian 2020] to maximize the transmission chances through static and semi-dynamic analyses. Researchers developed their circuit implementations [Dahlberg et al. 2019; DiAdamo et al. 2022] and new protocols for enhancing the reliability [Pirker and Dür 2019]. Chakraborty et al. [Chakraborty et al. 2019] provided an alternative protocol for distributed routing. Li et al. [Li et al. 2021] and Caleffi [Caleffi 2017] provide systems to improve transmission chances and message delivery rates. Buhrman and Röhrig [2003] examined the development of distributed quantum computing algorithms, and Cuomo et al. [2023] proposed an optimized compiler for distributed quantum computing.

Single-threaded Quantum Circuit Programming Languages. There are many single-location quantum circuit-based language development. Q# [Svore et al. 2018], Quilc [Smith et al. 2020], Scaffold [JavadiAbhari et al. 2015], Project Q [Steiger et al. 2018], Cirq [Google Quantum AI 2019], Qiskit [Aleksandrowicz et al. 2019] are industrial quantum circuit languages. There are formally verifying quantum circuit programs, including Qwire [Rand 2018], SQIR [Hietala et al. 2021], and QBricks [Chareton et al. 2021], quantum Hoare logic and its subsequent works [Liu et al. 2019; Ying 2012; Zhou et al. 2023], Qafny [Li et al. 2024]. These tools have been used to verify a range of quantum algorithms, from Grover's search to quantum phase estimation. There are works verifying quantum circuit optimizations (e.g., voQC [Hietala et al. 2023], CertiQ [Shi et al. 2019]), as well as verifying quantum circuit compilation procedures, including ReVerC [Amy et al. 2017] and ReQWIRE [Rand et al. 2018]. There are single-location circuit-based equivalence checkers [Chen et al. 2022; Peham et al. 2022; Shi et al. 2020; Sun and Wei 2022; Wang et al. 2022, 2021; Yamashita and Markov 2010] for verifying quantum compiler optimizations.

8 Conclusion and Future Work

We present `DisQ`, a system for expressing distributed quantum programs, which are user-specified rewrites of sequential programs. In `DisQ`, users can rewrite a sequential quantum program to a distributed one that can be executed in a remote distributed quantum system, and `DisQ` is able to verify their equivalence via the `DisQ` simulation mechanism. The benefit of such rewrites is to mitigate the restriction of entangled qubit sizes in single-location quantum computers, where we can utilize quantum networking techniques to allow a distributed quantum program to be executed on remote quantum computers where a large entanglement can be built.

We present `DisQ`'s formal syntax and semantics as a model for a distributed quantum system by combining the CHAM and MDP. We use a type system, with the type soundness, to guarantee that the execution of `DisQ` program is deadlock-free and represents quantum program behaviors. The `DisQ` simulation relation is developed based on equating sets of program configurations at the sequence points of quantum measurements, by summing the probabilities of different branches leading to the same outputs. We show by our case studies that the relation is capable of equating sequential quantum programs and their distributed versions.

Based on `DisQ`, we plan to rewrite different quantum algorithms into distributed versions and develop logical frameworks, such as temporal logics, on top of `DisQ` to reason about sophisticated distributed quantum systems.

9 Data-Availability Statement

The software that is mentioned in Section 5 and supports Section 6 as well as the Coq proofs for the theorems in Section 4, are available on Zenodo with DOI: [10.5281/zenodo.13924168](https://doi.org/10.5281/zenodo.13924168), and will be submitted for evaluation. The artifact is produced on the described experimental setting.

Acknowledgments

This material is based upon work supported by NSF under Award Number 2330974. This paper is dedicated to the memory of our dear co-author Rance Cleaveland.

References

- Gadi Aleksandrowicz, Thomas Alexander, Panagiotis Barkoutsos, Luciano Bello, Yael Ben-Haim, David Bucher, Francisco Jose Cabrera-Hernández, Jorge Carballo-Franquis, Adrian Chen, Chun-Fu Chen, Jerry M. Chow, Antonio D. Córcoles-Gonzales, Abigail J. Cross, Andrew Cross, Juan Cruz-Benito, Chris Culver, Salvador De La Puente González, Enrique De La Torre, Delton Ding, Eugene Dumitrescu, Ivan Duran, Pieter Eendebak, Mark Everitt, Ismael Faro Sertage, Albert Frisch, Andreas Fuhrer, Jay Gambetta, Borja Godoy Gago, Juan Gomez-Mosquera, Donny Greenberg, Ikko Hamamura, Vojtech Havlicek, Joe Hellmers, Lukasz Herok, Hiroshi Horii, Shaohan Hu, Takashi Imamichi, Toshinari Itoko, Ali Javadi-Abhari, Naoki Kanazawa, Anton Karazeev, Kevin Krsulich, Peng Liu, Yang Luh, Yunho Maeng, Manoel Marques, Francisco Jose Martin-Fernández, Douglas T. McClure, David McKay, Srujan Meesala, Antonio Mezzacapo, Nikolaj Moll, Diego Moreda Rodríguez, Giacomo Nannicini, Paul Nation, Pauline Ollitrault, Lee James O'Riordan, Hanhee Paik, Jesús Pérez, Anna Phan, Marco Pistoia, Viktor Prutyanov, Max Reuter, Julia Rice, Abdón Rodríguez Davila, Raymond Harry Putra Rudy, Mingi Ryu, Ninad Sathaye, Chris Schnabel, Eddie Schoute, Kanav Setia, Yunong Shi, Adenilton Silva, Yukio Siraichi, Seyon Sivarajah, John A. Smolin, Mathias Soeken, Hitomi Takahashi, Ivano Tavernelli, Charles Taylor, Pete Taylour, Kenso Trabling, Matthew Treinish, Wes Turner, Desiree Vogt-Lee, Christophe Vuillot, Jonathan A. Wildstrom, Jessica Wilson, Erick Winston, Christopher Wood, Stephen Wood, Stefan Wörner, Ismail Yunus Akhalwaya, and Christa Zoufal. 2019. Qiskit: An open-source framework for quantum computing. <https://doi.org/10.5281/zenodo.2562110>
- A. Ambainis. 2004. Quantum walk algorithm for element distinctness. In *45th Annual IEEE Symposium on Foundations of Computer Science*. 22–31. <https://doi.org/10.1109/FOCS.2004.54>
- Matthew Amy, Martin Roetteler, and Krysta M. Svore. 2017. Verified Compilation of Space-Efficient Reversible Circuits. In *Computer Aided Verification*, Rupak Majumdar and Viktor Kunčak (Eds.). Springer International Publishing, Cham, 3–21.
- Ebrahim Ardeshir-Larijani, Simon J. Gay, and Rajagopal Nagarajan. 2013. Equivalence Checking of Quantum Protocols. In *Tools and Algorithms for the Construction and Analysis of Systems*, Nir Piterman and Scott A. Smolka (Eds.). Springer Berlin Heidelberg, Berlin, Heidelberg, 478–492.

- Ebrahim Ardeshir-Larijani, Simon J. Gay, and Rajagopal Nagarajan. 2014. Verification of Concurrent Quantum Protocols by Equivalence Checking. In *Tools and Algorithms for the Construction and Analysis of Systems*, Erika Ábrahám and Klaus Havelund (Eds.). Springer Berlin Heidelberg, Berlin, Heidelberg, 500–514.
- David Barral, F. Javier Cardama, Guillermo Díaz, Daniel Faílde, Iago F. Llovo, Mariamo Mussa Juane, Jorge Vázquez-Pérez, Juan Villasuso, César Piñeiro, Natalia Costas, Juan C. Pichel, Tomás F. Pena, and Andrés Gómez. 2024. Review of Distributed Quantum Computing. From single QPU to High Performance Quantum Computing. arXiv:2404.01265 [quant-ph]
- Samik Basu, Madhavan Mukund, C. R. Ramakrishnan, I. V. Ramakrishnan, and Rakesh Verma. 2001. Local and Symbolic Bisimulation Using Tabled Constraint Logic Programming. In *Logic Programming*, Philippe Codognet (Ed.). Springer Berlin Heidelberg, Berlin, Heidelberg, 166–180.
- Robert Beals, Stephen Brierley, Oliver Gray, Aram W. Harrow, Samuel Kutin, Noah Linden, Dan Shepherd, and Mark Stather. 2013. Efficient distributed quantum computing. *Proceedings of the Royal Society A: Mathematical, Physical and Engineering Sciences* 469, 2153 (May 2013), 20120686. <https://doi.org/10.1098/rspa.2012.0686>
- Stephane Beauregard. 2003. Circuit for Shor’s Algorithm Using $2n+3$ Qubits. *Quantum Info. Comput.* 3, 2 (March 2003), 175–185.
- Charles H. Bennett, Gilles Brassard, Claude Crépeau, Richard Jozsa, Asher Peres, and William K. Wootters. 1993. Teleporting an unknown quantum state via dual classical and Einstein-Podolsky-Rosen channels. *Phys. Rev. Lett.* 70 (Mar 1993), 1895–1899. Issue 13. <https://doi.org/10.1103/PhysRevLett.70.1895>
- Charles H. Bennett and Stephen J. Wiesner. 1992. Communication via one- and two-particle operators on Einstein-Podolsky-Rosen states. *Phys. Rev. Lett.* 69 (Nov 1992), 2881–2884. Issue 20. <https://doi.org/10.1103/PhysRevLett.69.2881>
- Gérard Berry and Gérard Boudol. 1992. The chemical abstract machine. *Theoretical Computer Science* 96, 1 (1992), 217–248. [https://doi.org/10.1016/0304-3975\(92\)90185-1](https://doi.org/10.1016/0304-3975(92)90185-1)
- Harry Buhrman and Hein Röhrig. 2003. Distributed Quantum Computing. 1–20. https://doi.org/10.1007/978-3-540-45138-9_1
- Marcello Caleffi. 2017. Optimal Routing for Quantum Networks. *IEEE Access* 5 (2017), 22299–22312. <https://doi.org/10.1109/ACCESS.2017.2763325>
- Marcello Caleffi, Michele Amoretti, Davide Ferrari, Daniele Cuomo, Jessica Illiano, Antonio Manzalini, and Angela Sara Cacciapuoti. 2022. Distributed Quantum Computing: a Survey. (12 2022). arXiv:2212.10609 [quant-ph]
- Kaushik Chakraborty, Filip Rozpedek, Axel Dahlberg, and Stephanie Wehner. 2019. Distributed Routing in a Quantum Internet. <https://doi.org/10.48550/ARXIV.1907.11630>
- Christophe Charetton, Sébastien Bardin, François Bobot, Valentin Perrelle, and Benoît Valiron. 2021. An Automated Deductive Verification Framework for Circuit-building Quantum Programs. In *Programming Languages and Systems - 30th European Symposium on Programming, ESOP 2021, Held as Part of the European Joint Conferences on Theory and Practice of Software, ETAPS 2021, Luxembourg City, Luxembourg, March 27 - April 1, 2021, Proceedings (Lecture Notes in Computer Science, Vol. 12648)*, Nobuko Yoshida (Ed.). Springer, 148–177. https://doi.org/10.1007/978-3-030-72019-3_6
- Tian-Fu Chen, Jie-Hong R. Jiang, and Min-Hsiu Hsieh. 2022. Partial Equivalence Checking of Quantum Circuits. In *2022 IEEE International Conference on Quantum Computing and Engineering (QCE)*. IEEE. <https://doi.org/10.1109/qce53715.2022.00082>
- Wentao Chen, Yao Lu, Shuaining Zhang, Kuan Zhang, Guan hao Huang, Mu Qiao, Xiaolu Su, Jialiang Zhang, Jing-Ning Zhang, Leonardo Bianchi, M. S. Kim, and Kihwan Kim. 2023. Scalable and programmable phononic network with trapped ions. *Nature Physics* 19, 6 (01 Jun 2023), 877–883. <https://doi.org/10.1038/s41567-023-01952-5>
- Andrew Childs, Ben Reichardt, Robert Spalek, and Shengyu Zhang. 2007. Every NAND formula of size N can be evaluated in time $N^{1/2+o(1)}$ on a Quantum Computer. (03 2007).
- Cheng Chu, Zhenxiao Fu, Yilun Xu, Gang Huang, Hausi Muller, Fan Chen, and Lei Jiang. 2024. TITAN: A Distributed Large-Scale Trapped-Ion NISQ Computer. arXiv:2402.11021 [quant-ph] <https://arxiv.org/abs/2402.11021>
- Steven Cuccaro, Thomas Draper, Samuel Kutin, and David Moulton. 2004. A new quantum ripple-carry addition circuit. (11 2004).
- Daniele Cuomo, Marcello Caleffi, and Angela Sara Cacciapuoti. 2020. Towards a distributed quantum computing ecosystem. *IET Quantum Communication* 1, 1 (July 2020), 3–8. <https://doi.org/10.1049/iet-qtc.2020.0002>
- Daniele Cuomo, Marcello Caleffi, Kevin Krsulich, Filippo Tramonto, Gabriele Agliardi, Enrico Prati, and Angela Sara Cacciapuoti. 2023. Optimized Compiler for Distributed Quantum Computing. *ACM Transactions on Quantum Computing* 4, 2, Article 15 (feb 2023), 29 pages. <https://doi.org/10.1145/3579367>
- Axel Dahlberg, Matthew Skrzypczyk, Tim Coopmans, Leon Wubben, Filip Rozpundek, Matteo Pompili, Arian Stolk, Przemysław Pawełczak, Robert Knegjens, Julio de Oliveira Filho, Ronald Hanson, and Stephanie Wehner. 2019. A Link Layer Protocol for Quantum Networks. In *Proceedings of the ACM Special Interest Group on Data Communication (Beijing, China) (SIGCOMM ’19)*. Association for Computing Machinery, New York, NY, USA, 159–173. <https://doi.org/10.1145/3341302.3342070>

- Zohreh Davarzani, Mariam Zomorodi, and Mahboobeh Houshmand. 2022. A Hierarchical Approach For Building Distributed Quantum Systems. *Scientific Reports* 12 (09 2022). <https://doi.org/10.1038/s41598-022-18989-w>
- Tim Davidson, Simon Gay, H. Mlnářik, Rajagopal Nagarajan, and Nick Papanikolaou. 2012. Model Checking for Communicating Quantum Processes. *International Journal of Unconventional Computing* 8 (01 2012), 73–98.
- Stephen DiAdamo, Marco Ghibaudi, and James Cruise. 2021. Distributed Quantum Computing and Network Control for Accelerated VQE. *IEEE Transactions on Quantum Engineering* 2 (2021), 1–21. <https://doi.org/10.1109/tqe.2021.3057908>
- Stephen DiAdamo, Bing Qi, Glen Miller, Ramana Kompella, and Alireza Shabani. 2022. Packet switching in quantum networks: A path to the quantum Internet. *Phys. Rev. Res.* 4 (Oct 2022), 043064. Issue 4. <https://doi.org/10.1103/PhysRevResearch.4.043064>
- Paul Adrien Maurice Dirac. 1939. A new notation for quantum mechanics. *Mathematical Proceedings of the Cambridge Philosophical Society* 35 (1939), 416 – 418.
- J. Eisert, K. Jacobs, P. Papadopoulos, and M. B. Plenio. 2000. Optimal local implementation of nonlocal quantum gates. *Phys. Rev. A* 62 (Oct 2000), 052317. Issue 5. <https://doi.org/10.1103/PhysRevA.62.052317>
- Yuan Feng, Runyao Duan, and Mingsheng Ying. 2012. Bisimulation for Quantum Processes. *ACM Trans. Program. Lang. Syst.* 34, 4, Article 17 (dec 2012), 43 pages. <https://doi.org/10.1145/2400676.2400680>
- Yuan Feng, Sanjiang Li, and Mingsheng Ying. 2022. Verification of Distributed Quantum Programs. *ACM Trans. Comput. Logic* 23, 3, Article 19 (apr 2022), 40 pages. <https://doi.org/10.1145/3517145>
- Simon Gay, Rajagopal Nagarajan, and Nikolaos Papanikolaou. 2013. Specification and Verification of Quantum Protocols. *Semantic Techniques in Quantum Computation* (01 2013). <https://doi.org/10.1017/CBO9781139193313.012>
- Simon J. Gay and Rajagopal Nagarajan. 2005. Communicating Quantum Processes. In *Proceedings of the 32nd ACM SIGPLAN-SIGACT Symposium on Principles of Programming Languages* (Long Beach, California, USA) (POPL '05). Association for Computing Machinery, New York, NY, USA, 145–157. <https://doi.org/10.1145/1040305.1040318>
- Radu-Iulian Gheorghica. 2023. An Algorithm for Concurrent Use of Quantum Simulators and Computers in the Context of Subgraph Isomorphism. In *2023 IEEE 17th International Symposium on Applied Computational Intelligence and Informatics (SACI)*. 000721–000726. <https://doi.org/10.1109/SACI58269.2023.10158547>
- Thomas Gibson-Robinson, Alexandre Boulgakov Philip Armstrong, and A.W. Roscoe. 2014. FDR3 - A Modern Refinement Checker for CSP. In *TACAS*. In Press.
- Google Quantum AI. 2019. Cirq: An Open Source Framework for Programming Quantum Computers. <https://quantumai.google/cirq>
- Fabrizio Granelli, Riccardo Bassoli, Janis Nötzel, Frank Fitzek, Holger Boche, and Nelson Fonseca. 2022. A Novel Architecture for Future Classical-Quantum Communication Networks. *Wireless Communications and Mobile Computing* 2022 (04 2022), 1–18. <https://doi.org/10.1155/2022/3770994>
- Daniel M. Greenberger, Michael A. Horne, and Anton Zeilinger. 1989. *Going beyond Bell's Theorem*. Springer Netherlands, Dordrecht, 69–72. https://doi.org/10.1007/978-94-017-0849-4_10
- Salman Haider and Dr. Syed Asad Raza Kazmi. 2020. An extended quantum process algebra (eQPA) approach for distributed quantum systems. arXiv:2001.04249 [cs.LO]
- Thomas Häner, Vadym Kliuchnikov, Martin Roetteler, Mathias Soeken, and Alexander Vaschillo. 2022. QParallel: Explicit Parallelism for Programming Quantum Computers. (10 2022). arXiv:2210.03680 [quant-ph]
- Thomas Häner, Martin Roetteler, and Krysta M. Svore. 2017. Factoring Using $2n + 2$ Qubits with Toffoli Based Modular Multiplication. *Quantum Info. Comput.* 17, 7–8 (June 2017), 673–684.
- Thomas Häner, Damian S. Steiger, Torsten Hoefler, and Matthias Troyer. 2021. Distributed quantum computing with QMPI. In *Proceedings of the International Conference for High Performance Computing, Networking, Storage and Analysis* (, St. Louis, Missouri,) (SC '21). Association for Computing Machinery, New York, NY, USA, Article 16, 13 pages. <https://doi.org/10.1145/3458817.3476172>
- Kesha Hietala, Robert Rand, Shih-Han Hung, Liyi Li, and Michael Hicks. 2021. Proving Quantum Programs Correct. In *Proceedings of the Conference on Interactive Theorem Proving (ITP)*.
- Kesha Hietala, Robert Rand, Liyi Li, Shih-Han Hung, Xiaodi Wu, and Michael Hicks. 2023. A Verified Optimizer for Quantum Circuits. *ACM Trans. Program. Lang. Syst.* 45, 3, Article 18 (Sept. 2023), 35 pages. <https://doi.org/10.1145/3604630>
- Stefan Hillmich, Alwin Zulehner, and Robert Wille. 2020. Concurrency in DD-based Quantum Circuit Simulation. In *2020 25th Asia and South Pacific Design Automation Conference (ASP-DAC)*. 115–120. <https://doi.org/10.1109/ASP-DAC47756.2020.9045711>
- C. A. R. Hoare. 1985. *Communicating sequential processes*. Prentice-Hall, Inc., Upper Saddle River, NJ, USA.
- Photonic Inc. , Francis Afzal, Mohsen Akhlaghi, Stefanie J. Beale, Olinka Bedroya, Kristin Bell, Laurent Bergeron, Kent Bonsma-Fisher, Polina Bychkova, Zachary M. E. Chaisson, Camille Chartrand, Chloe Clear, Adam Darcie, Adam DeAbreu, Colby DeLisle, Lesley A. Duncan, Chad Dundas Smith, John Dunn, Amir Ebrahimi, Nathan Evetts, Daker Fernandes Pinheiro, Patricio Fuentes, Tristen Georgiou, Biswarup Guha, Rafael Haenel, Daniel Higginbottom, Daniel M. Jackson, Navid Jahed, Amin Khorshidahmad, Prasoon K. Shandilya, Alexander T. K. Kurkjian, Nikolai Lauk, Nicholas R. Lee-Hone,

- Eric Lin, Rostyslav Litynskyy, Duncan Lock, Lisa Ma, Iain MacGilp, Evan R. MacQuarrie, Aaron Mar, Alireza Marefat Khah, Alex Matiash, Evan Meyer-Scott, Cathryn P. Michaels, Juliana Motira, Narwan Kabir Noori, Egor Ospadov, Ekta Patel, Alexander Patscheider, Danny Paulson, Ariel Petruk, Adarsh L. Ravindranath, Bogdan Reznichenko, Myles Ruether, Jeremy Ruscica, Kunal Saxena, Zachary Schaller, Alex Seidlitz, John Senger, Youn Seok Lee, Orbel Sevoyan, Stephanie Simmons, Oney Soykal, Leea Stott, Quyen Tran, Spyros Tserkis, Ata Ulhaq, Wyatt Vine, Russ Weeks, Gary Wolfowicz, and Isao Yoneda. 2024a. Distributed Quantum Computing in Silicon. arXiv:2406.01704 [quant-ph] <https://arxiv.org/abs/2406.01704>
- Photonic Inc, ; Francis Afzal, Mohsen Akhlaghi, Stefanie J. Beale, Olinka Bedroya, Kristin Bell, Laurent Bergeron, Kent Bonsma-Fisher, Polina Bychkova, Zachary M. E. Chaisson, Camille Chartrand, Chloe Clear, Adam Darcie, Adam DeAbreu, Colby DeLisle, Lesley A. Duncan, Chad Dundas Smith, John Dunn, Amir Ebrahimi, Nathan Evetts, Daker Fernandes Pinheiro, Patricio Fuentes, Tristen Georgiou, Biswarup Guha, Rafael Haenel, Daniel Higginbottom, Daniel M. Jackson, Navid Jahed, Amin Khorshidahmad, Prason K. Shandilya, Alexander T. K. Kurkjian, Nikolai Lauk, Nicholas R. Lee-Hone, Eric Lin, Rostyslav Litynskyy, Duncan Lock, Lisa Ma, Iain MacGilp, Evan R. MacQuarrie, Aaron Mar, Alireza Marefat Khah, Alex Matiash, Evan Meyer-Scott, Cathryn P. Michaels, Juliana Motira, Narwan Kabir Noori, Egor Ospadov, Ekta Patel, Alexander Patscheider, Danny Paulson, Ariel Petruk, Adarsh L. Ravindranath, Bogdan Reznichenko, Myles Ruether, Jeremy Ruscica, Kunal Saxena, Zachary Schaller, Alex Seidlitz, John Senger, Youn Seok Lee, Orbel Sevoyan, Stephanie Simmons, Oney Soykal, Leea Stott, Quyen Tran, Spyros Tserkis, Ata Ulhaq, Wyatt Vine, Russ Weeks, Gary Wolfowicz, and Isao Yoneda. 2024b. Distributed Quantum Computing in Silicon. arXiv:2406.01704 [quant-ph]
- IonQ. 2024. *IonQ Demonstrates Remote Ion-Ion Entanglement, a Significant Milestone in Developing Networked Quantum Systems at Scale*. <https://ionq.com/news/ionq-demonstrates-remote-ion-ion-entanglement-a-significant-milestone-in>
- Ali JavadiAbhari, Shruti Patil, Daniel Kudrow, Jeff Heckey, Alexey Lvov, Frederic T. Chong, and Margaret Martonosi. 2015. ScaffCC: Scalable compilation and analysis of quantum programs. *Parallel Comput.* 45 (June 2015), 2–17. <https://doi.org/10.1016/j.parco.2014.12.001>
- Philippe Jorrand and Marie Lalire. 2004. Toward a Quantum Process Algebra. In *Proceedings of the 1st Conference on Computing Frontiers (Ischia, Italy) (CF '04)*. Association for Computing Machinery, New York, NY, USA, 111–119. <https://doi.org/10.1145/977091.977108>
- B. Juliá-Díaz, Joseph Burdis, and Frank Tabakin. 2005. QDENSIT—a mathematica quantum computer simulation. *Computer Physics Communications* 180 (08 2005), 914–934. <https://doi.org/10.1016/j.cpc.2005.12.021>
- Wojciech Kozłowski, Axel Dahlberg, and Stephanie Wehner. 2020. Designing a Quantum Network Protocol. In *Proceedings of the 16th International Conference on Emerging Networking Experiments and Technologies (Barcelona, Spain) (CoNEXT '20)*. Association for Computing Machinery, New York, NY, USA, 1–16. <https://doi.org/10.1145/3386367.3431293>
- Dario Lago-Rivera, Jelena V. Rakonjac, Samuele Grandi, and Hugues de Riedmatten. 2023. Long distance multiplexed quantum teleportation from a telecom photon to a solid-state qubit. *Nature Communications* 14, 1 (05 Apr 2023), 1889. <https://doi.org/10.1038/s41467-023-37518-5>
- Jian Li, Mingjun Wang, Qidong Jia, Kaiping Xue, Nenghai Yu, Qibin Sun, and Jun Lu. 2021. Fidelity-Guarantee Entanglement Routing in Quantum Networks. <https://doi.org/10.48550/ARXIV.2111.07764>
- Liyi Li, Finn Voichick, Kesha Hietala, Yuxiang Peng, Xiaodi Wu, and Michael Hicks. 2022. Verified Compilation of Quantum Oracles. In *OOPSLA 2022*. <https://doi.org/10.48550/ARXIV.2112.06700>
- Liyi Li, Mingwei Zhu, Rance Cleaveland, Alexander Nicoletti, Yi Lee, Le Chang, and Xiaodi Wu. 2024. Qafny: A Quantum-Program Verifier. In *ECOOP 2024*.
- Junyi Liu, Bohua Zhan, Shuling Wang, Shenggang Ying, Tao Liu, Yangjia Li, Mingsheng Ying, and Naijun Zhan. 2019. Formal Verification of Quantum Algorithms Using Quantum Hoare Logic. In *Computer Aided Verification*, Isil Dillig and Serdar Tasiran (Eds.). Springer International Publishing, Cham, 187–207.
- Formal Systems (Europe) Ltd. 2010. Failures-Divergence Refinement. FDR2 User Manual. In *FDR2 User Manual*.
- Frédéric Magniez, Miklos Santha, and Mario Szegedy. 2005. Quantum Algorithms for the Triangle Problem. In *Proceedings of the Sixteenth Annual ACM-SIAM Symposium on Discrete Algorithms (Vancouver, British Columbia) (SODA '05)*. Society for Industrial and Applied Mathematics, USA, 1109–1117.
- D. Main, P. Drmota, D. P. Nadlinger, E. M. Ainley, A. Agrawal, B. C. Nichol, R. Srinivas, G. Araneda, and D. M. Lucas. 2024. Distributed Quantum Computing across an Optical Network Link. arXiv:2407.00835 [quant-ph] <https://arxiv.org/abs/2407.00835>
- Ryan Mandelbaum, Robert Davis, Jennifer Janecek, and Rafi Letzter. 2023. You need 100 qubits to accelerate discovery with quantum. <https://www.ibm.com/quantum/blog/100-qubit-utility>
- Andrey Markov. 1906. Rasprostraneniye zakona bol'shih chisel na velichiny, zavisyaschie drug ot druga. *Izvestiya Fiziko-matematicheskogo obschestva pri Kazanskom universitete* 15 (1906), 135–156.
- Andrey Markov. 1907. Extension of the Limit Theorems of Probability Theory to a Sum of Variables Connected in a chain. *The Notes of the Imperial Academy of Sciences of St. Petersburg VIII Series, Physio-Mathematical College XXII/9* (1907).

- R. Van Meter and S. J. Devitt. 2016. The Path to Scalable Distributed Quantum Computing. *Computer* 49, 09 (sep 2016), 31–42. <https://doi.org/10.1109/MC.2016.291>
- Robin Milner. 1980. *A Calculus of Communicating Systems*. Springer Berlin, Heidelberg.
- Robin Milner, Joachim Parrow, and David Walker. 1992. A calculus of mobile processes, I. *Information and Computation* 100, 1 (1992), 1–40. [https://doi.org/10.1016/0890-5401\(92\)90008-4](https://doi.org/10.1016/0890-5401(92)90008-4)
- Sreraman Muralidharan. 2024. The simulation of distributed quantum algorithms. arXiv:2402.10745 [quant-ph]
- Michael A. Nielsen and Isaac L. Chuang. 2011. *Quantum Computation and Quantum Information* (10th anniversary ed.). Cambridge University Press, USA.
- Karmela Padavic-Callaghan. 2023. *Record-breaking Number of Qubits Entangled In a Quantum Computer*. <https://www.newscientist.com/article/2382022-record-breaking-number-of-qubits-entangled-in-a-quantum-computer/>
- Rhea Parekh, Andrea Ricciardi, Ahmed Darwish, and Stephen DiAdamo. 2021. Quantum Algorithms and Simulation for Parallel and Distributed Quantum Computing. In *2021 IEEE/ACM Second International Workshop on Quantum Computing Software (QCS)*. 9–19. <https://doi.org/10.1109/QCS54837.2021.00005>
- Tom Peham, Lukas Burgholzer, and Robert Wille. 2022. Equivalence Checking of Quantum Circuits With the ZX-Calculus. *IEEE Journal on Emerging and Selected Topics in Circuits and Systems* 12, 3 (Sept. 2022), 662–675. <https://doi.org/10.1109/jetcas.2022.3202204>
- S. Pirandola, J. Eisert, C. Weedbrook, A. Furusawa, and S. L. Braunstein. 2015. Advances in quantum teleportation. *Nature Photonics* 9, 10 (01 Oct 2015), 641–652. <https://doi.org/10.1038/nphoton.2015.154>
- Stefano Pirandola, Riccardo Laurenza, Carlo Ottaviani, and Leonardo Banchi. 2017. Fundamental limits of repeaterless quantum communications. *Nature Communications* 8 (04 2017), 15043. <https://doi.org/10.1038/ncomms15043>
- A Pirker and W Dür. 2019. A quantum network stack and protocols for reliable entanglement-based networks. *New Journal of Physics* 21, 3 (mar 2019), 033003. <https://doi.org/10.1088/1367-2630/ab05f7>
- Martin L. Puterman. 1994. *Markov Decision Processes: Discrete Stochastic Dynamic Programming* (1st ed.). John Wiley & Sons, Inc., USA.
- Matthew Pysher, Alon Bahabad, Peng Peng, Ady Arie, and Olivier Pfister. 2010. Quasi-phase-matched concurrent nonlinearities in periodically poled KTiOPO4 for quantum computing over the optical frequency comb. *Opt. Lett.* 35, 4 (Feb 2010), 565–567. <https://doi.org/10.1364/OL.35.000565>
- Xudong Qin, Yuxin Deng, and Wenjie Du. 2020. Verifying Quantum Communication Protocols with Ground Bisimulation. In *Tools and Algorithms for the Construction and Analysis of Systems*, Armin Biere and David Parker (Eds.). Springer International Publishing, Cham, 21–38.
- Robert Rand. 2018. *Formally verified quantum programming*. Ph.D. Dissertation. University of Pennsylvania.
- Robert Rand, Jennifer Paykin, Dong-Ho Lee, and S. Zdancewic. 2018. ReQWIRE: Reasoning about Reversible Quantum Circuits. In *QPL*.
- Gustavo Rigolin. 2005. Quantum teleportation of an arbitrary two-qubit state and its relation to multipartite entanglement. *Physical Review A* 71, 3 (mar 2005). <https://doi.org/10.1103/physreva.71.032303>
- Davide Sangiorgi. 1993. A Theory of Bisimulation for the pi-Calculus. In *CONCUR (Lecture Notes in Computer Science, Vol. 715)*, Eike Best (Ed.). Springer, 127–142.
- Shouqian Shi and Chen Qian. 2020. Concurrent Entanglement Routing for Quantum Networks: Model and Designs. In *Proceedings of the Annual Conference of the ACM Special Interest Group on Data Communication on the Applications, Technologies, Architectures, and Protocols for Computer Communication (Virtual Event, USA) (SIGCOMM '20)*. Association for Computing Machinery, New York, NY, USA, 62–75. <https://doi.org/10.1145/3387514.3405853>
- Yunong Shi, Xupeng Li, Runzhou Tao, Ali Javadi-Abhari, Andrew W. Cross, Frederic T. Chong, and Ronghui Gu. 2019. Contract-based verification of a realistic quantum compiler. *arXiv e-prints* (Aug 2019). arXiv:1908.08963 [quant-ph]
- Yunong Shi, Runzhou Tao, Xupeng Li, Ali Javadi-Abhari, Andrew W. Cross, Frederic T. Chong, and Ronghui Gu. 2020. CertiQ: A Mostly-automated Verification of a Realistic Quantum Compiler. arXiv:1908.08963 [quant-ph]
- P.W. Shor. 1994. Algorithms for quantum computation: discrete logarithms and factoring. In *Proceedings 35th Annual Symposium on Foundations of Computer Science*. 124–134. <https://doi.org/10.1109/SFCS.1994.365700>
- Robert S. Smith, Eric C. Peterson, Mark G. Skilbeck, and Erik J. Davis. 2020. An Open-Source, Industrial-Strength Optimizing Compiler for Quantum Programs. arXiv:2003.13961 [quant-ph]
- Damian S. Steiger, Thomas Häner, and Matthias Troyer. 2018. ProjectQ: an open source software framework for quantum computing. *Quantum* 2 (Jan. 2018), 49. <https://doi.org/10.22331/q-2018-01-31-49>
- Weixiao Sun and Zhaohui Wei. 2022. Equivalence checking of quantum circuits by nonlocality. *npj Quantum Information* 8, 1 (29 Nov 2022), 139. <https://doi.org/10.1038/s41534-022-00652-x>
- Krysta Svore, Alan Geller, Matthias Troyer, John Azariah, Christopher Granade, Bettina Heim, Vadym Kliuchnikov, Mariia Mykhailova, Andres Paz, and Martin Roetteler. 2018. Q#: Enabling Scalable Quantum Computing and Development with a High-level DSL. In *Proceedings of the Real World Domain Specific Languages Workshop 2018 (RWDSL2018)*. ACM. <https://doi.org/10.1145/3183895.3183901>

- Matt Swayne. 2024. *Google Is Looking For Proposals to Push Boundaries in Distributed Quantum Computing*. <https://thequantuminsider.com/2024/06/18/google-is-looking-for-proposals-to-push-boundaries-in-distributed-quantum-computing/>
- Anya Taffioviich and Eric C.R. Hehner. 2009. Programming with Quantum Communication. *Electronic Notes in Theoretical Computer Science* 253, 3 (2009), 99–118. <https://doi.org/10.1016/j.entcs.2009.10.008> Proceedings of Seventh Workshop on Quantitative Aspects of Programming Languages (QAPL 2009).
- Wei Tang and Margaret Martonosi. 2024. Distributed Quantum Computing via Integrating Quantum and Classical Computing. *Computer* 57, 4 (2024), 131–136. <https://doi.org/10.1109/MC.2024.3360569>
- Qisheng Wang, Riling Li, and Mingsheng Ying. 2022. Equivalence Checking of Sequential Quantum Circuits. *IEEE Transactions on Computer-Aided Design of Integrated Circuits and Systems* 41, 9 (Sept. 2022), 3143–3156. <https://doi.org/10.1109/tcad.2021.3117506>
- Qisheng Wang, Junyi Liu, and Mingsheng Ying. 2021. Equivalence checking of quantum finite-state machines. *J. Comput. System Sci.* 116 (March 2021), 1–21. <https://doi.org/10.1016/j.jcss.2020.08.004>
- Stephanie Wehner, David Elkouss, and Ronald Hanson. 2018. Quantum internet: A vision for the road ahead. *Science* 362, 6412 (2018), eaam9288. <https://doi.org/10.1126/science.aam9288> arXiv:<https://www.science.org/doi/pdf/10.1126/science.aam9288>
- Ligang Xiao, Daowen Qiu, Le Luo, and Paulo Mateus. 2023. Distributed Shor’s algorithm. *Quantum Information and Computation* 23 (01 2023), 27–44. <https://doi.org/10.26421/QIC23.1-2-3>
- Shigeru Yamashita and Igor L. Markov. 2010. Fast equivalence-checking for quantum circuits. In *2010 IEEE/ACM International Symposium on Nanoscale Architectures*. 23–28. <https://doi.org/10.1109/NANOARCH.2010.5510932>
- Bao Yan, Ziqi Tan, Shijie Wei, Haocong Jiang, Weilong Wang, Hong Wang, Lan Luo, Qianheng Duan, Yiting Liu, Wenhao Shi, Yangyang Fei, Xiangdong Meng, Yu Han, Zheng Shan, Jiachen Chen, Xuhao Zhu, Chuanyu Zhang, Feitong Jin, Hekang Li, Chao Song, Zhen Wang, Zhi Ma, H. Wang, and Gui-Lu Long. 2022. Factoring integers with sublinear resources on a superconducting quantum processor. arXiv:2212.12372 [quant-ph]
- Anocha Yimsiriwattana and Samuel J. Lomonaco Jr. 2004. Distributed quantum computing: a distributed Shor algorithm. In *Quantum Information and Computation II*, Eric Donkor, Andrew R. Pirich, and Howard E. Brandt (Eds.). SPIE. <https://doi.org/10.1117/12.546504>
- Mingsheng Ying. 2012. Floyd–Hoare Logic for Quantum Programs. *ACM Trans. Program. Lang. Syst.* 33, 6, Article 19 (Jan. 2012), 49 pages. <https://doi.org/10.1145/2049706.2049708>
- Mingsheng Ying and Yuan Feng. 2009. An Algebraic Language for Distributed Quantum Computing. *IEEE Trans. Comput.* 58, 6 (2009), 728–743. <https://doi.org/10.1109/TC.2009.13>
- Mingsheng Ying, Yuan Feng, Runyao Duan, and Zhengfeng Ji. 2009. An Algebra of Quantum Processes. *ACM Trans. Comput. Logic* 10, 3, Article 19 (apr 2009), 36 pages. <https://doi.org/10.1145/1507244.1507249>
- Mingsheng Ying, Li Zhou, and Yangjia Li. 2018. Reasoning about Parallel Quantum Programs. arXiv:1810.11334
- Mingsheng Ying, Li Zhou, Yangjia Li, and Yuan Feng. 2022. A proof system for disjoint parallel quantum programs. *Theoretical Computer Science* 897 (2022), 164–184. <https://doi.org/10.1016/j.tcs.2021.10.025>
- Zhicheng Zhang and Mingsheng Ying. 2024. Atomicity in Distributed Quantum Computing. arXiv:2404.18592 [quant-ph]
- Li Zhou, Gilles Barthe, Pierre-Yves Strub, Junyi Liu, and Mingsheng Ying. 2023. CoqQ: Foundational Verification of Quantum Programs. *Proc. ACM Program. Lang.* 7, POPL, Article 29 (jan 2023), 33 pages. <https://doi.org/10.1145/3571222>

A Full Syntax and More Semantics for The DisQ Language

Unitary Expr	μ	
Bool Expr	B	
Local Action	$A ::= \kappa \leftarrow \mu \mid x \leftarrow \mathcal{M}^{[l]}(\kappa) \mid \nu x(n)$	
Communication Action	$D ::= a!v \mid a?(y)$	
Process	$R, T ::= 0 \mid D.R \mid A.R \mid \text{if } (B) R \text{ else } T$	
Membrane	$P, Q ::= \{\bar{R}\}_l \mid R\{\bar{T}\}_l \mid \nu x(n).P \mid \partial c(n).P$	

$\frac{\text{S-NEWVARP} \quad \text{loc}(P) = l}{(\Phi, \nu x(n).P) \xrightarrow{l,1} (\Phi \cup \{x[0, n]\}_l \mapsto \bar{0}\rangle, P)}$	$\text{S-NEWVARR} \quad (\varphi, \nu x(n).R) \xrightarrow{1} (\varphi \cup \{x[0, n]\}_l \mapsto \bar{0}\rangle, R)$
--	--

$\frac{\text{T-NEWP} \quad \text{loc}(P) = l \quad \Omega(l)[x \mapsto Q(n)]; \Sigma \cup \{x[0, n]\}_l : \text{EN} \vdash P \triangleright \Sigma'}{\Omega; \Sigma \vdash \nu x(n).P \triangleright \Sigma'}$	$\frac{\text{T-NEWR} \quad \Omega(l)[x \mapsto Q(n)]; \sigma \cup \{x[0, n]\} : \text{EN} \vdash P \triangleright \sigma'}{\Omega; \sigma \vdash_l \nu x(n).R \triangleright \sigma'}$
--	--

$\frac{\text{T-PARM} \quad \Sigma \leq \Sigma' \quad \Omega; \Sigma' \vdash P \triangleright \Sigma''}{\Omega; \Sigma_1 \cup \Sigma \vdash P \triangleright \Sigma_1 \cup \Sigma''}$	$\frac{\text{T-PAR} \quad \sigma \leq \sigma' \quad \Omega; \sigma' \vdash e \triangleright \sigma''}{\Omega; \sigma_1 \cup \sigma \vdash e \triangleright \sigma_1 \cup \sigma''}$
--	---

Fig. 12. DisQ complete syntax, additional semantic and type rules. Marked red parts are new syntax.

In Figure 12, we add the $\nu x(n)$ operations in the process and membrane level to generate a blank array (x) of size n . Rule S-NEWVARP introduces a new blank n -qubit quantum array in the membrane l , and rule S-NEWVARR introduces a new blank n -qubit quantum array in the process R . The type rules T-PAR and T-PARM perform equivalence rewrites as typing relationships in the process and membrane levels, respectively.

A.1 DisQ Equivalence Relations

The DisQ type system maintains simultaneity through the type-guided state rewrites, formalized as equivalence relations (Figure 14). The equivalence relations happen in our type rules T-PAR and T-PARM in Figure 12. We only show the rewrite rules for local loci, and the loci with membrane structures can be manipulated through the merged rules in Figure 2, as well as a similar style of permutation rules in Section 4.3. Other than the locus qubit position permutation being introduced, the types below associated with loci in the environment also play an essential role in the rewrites.

Quantum Type	$\tau ::=$	$\text{Nor} \mid \text{Had} \mid \text{EN}$
Quantum Value (Forms)	$q ::=$	$w \mid \frac{1}{\sqrt{2^n}} \otimes_{j=0}^{n-1} (0\rangle + \alpha(r_j) 1\rangle) \mid \sum_{j=0}^m w_j$

The DisQ type system is inherited from the QAFNY type system [Li et al. 2024] with three different types. Quantum values are categorized into three different types: Nor, Had and EN. A *normal* value (Nor) is an array (tensor product) of single-qubit values $|0\rangle$ or $|1\rangle$. Sometimes, a (Nor)-typed value is associated with an amplitude z , representing an intermediate partial program

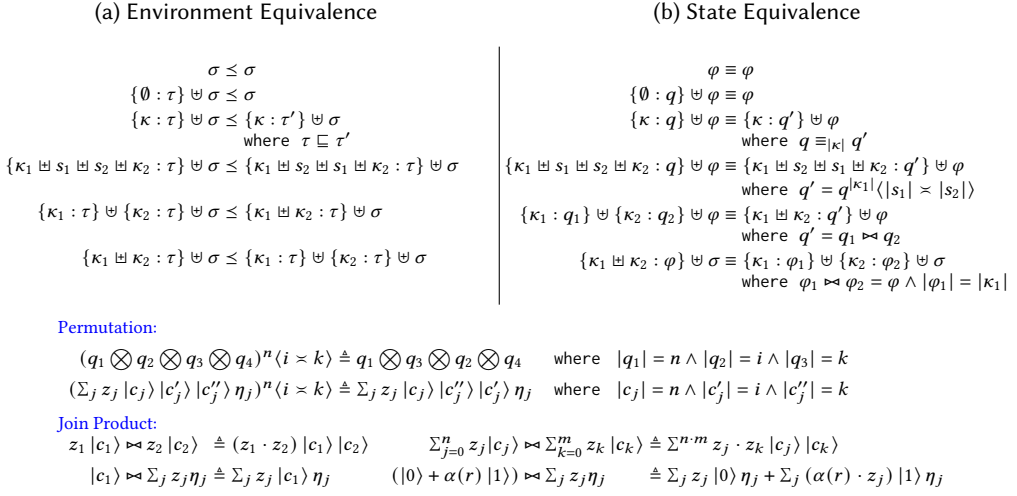


Fig. 13. DisQ type/state relations. \cdot is math mult. Term $\sum^{n-m} P$ is a summation omitting the indexing details. \otimes expands a Had array, as $\frac{1}{\sqrt{2^{n+m}}} \otimes_{j=0}^{n+m-2} q_j = (\frac{1}{\sqrt{2^n}} \otimes_{j=0}^{n-1} q_j) \otimes (\frac{1}{\sqrt{2^m}} \otimes_{j=0}^{m-1} q_j)$.

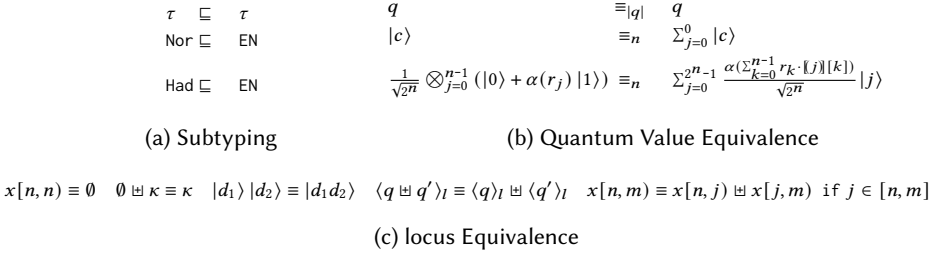


Fig. 14. DisQ type/state relations.

state. A *Hadamard* (Had) typed value represents a collection of qubits in superposition but not entangled, i.e., an n -qubit array $\frac{1}{\sqrt{2}}(|0\rangle + \alpha(r_0) |1\rangle) \otimes \dots \otimes \frac{1}{\sqrt{2}}(|0\rangle + \alpha(r_{n-1}) |1\rangle)$, can be encoded as $\frac{1}{\sqrt{2^n}} \otimes_{j=0}^{n-1} (|0\rangle + \alpha(r_j) |1\rangle)$, with $\alpha(r_j) = e^{2\pi i r_j}$ ($r_j \in \mathbb{R}$) being the *local phase*, a special amplitude whose norm is 1, i.e., $|\alpha(r_j)| = 1$. The most general form of n -qubit values is the *entanglement* (EN) typed value, consisting of a linear combination (represented as an array) of basis-kets, as $\sum_{j=0}^m z_j \beta_j \eta_j$, where m is the number of elements in the array. In DisQ, we *extend* traditional basis-ket structures in the Dirac notation to be the above form, so each basis-ket of the above value contains not only an amplitude z_j and a basis β_j but also a frozen basis stack η_j , storing bases not directly involved in the current computation. Here, β_j can always be represented as a single $|c_j\rangle$ by the equation in Figure 2. Every β_j in the array has the same cardinality, e.g., if $|c_0| = n$ ($\beta_0 = |c_0\rangle$), then $|c_i| = n$ ($\beta_j = |c_j\rangle$) for all j .

In DisQ, a locus represents a possibly entangled qubit group. From the study of many quantum algorithms [Ambainis 2004; Beauregard 2003; Childs et al. 2007; Häner et al. 2017; Magniez et al. 2005; Nielsen and Chuang 2011; Rigolin 2005; Shor 1994], we found that the establishment of an entanglement group can be viewed as a loop structure of incrementally adding a qubit to the group

at a time, representing the entanglement's scope expansion. This behavior is similar to splits and joins of array elements if we view quantum states as arrays. However, joining and splitting two EN-typed values are hard problems⁴. Another critical observation in studying many quantum algorithms is that the entanglement group establishment usually involves splitting a qubit in a Nor/Had typed value and joining it to an existing EN typed entanglement group. We manage these join and split patterns type-guided equations in DISQ, suitable for automated verification.

The semantics in Figure 6 assumes that the loci in quantum states can be in ideal forms, e.g., rule S-OP assumes that the target locus κ are always prefixed. This step is valid if we can rewrite (type environment partial order \leq) the locus to the ideal form through rule T-PAR and T-PARM in Figure 8, which interconnectively rewrites the locus appearing in the state, through our state equivalence relation (\equiv), as the locus state simultaneity enforcement. The state equivalence rewrites have two components.

First, the type and quantum value forms have simultaneity in Figure 14, i.e., given a type τ_1 for a locus κ in a type environment (Σ), if it is a subtype (\sqsubseteq) of another type τ_2 , K 's value q_1 in a state (Φ) can be rewritten to q_2 that has the type τ_2 through state equivalence rewrites (\equiv_n) where n is the number of qubits in q_1 and q_2 . Both \sqsubseteq and \equiv_n are reflexive and types Nor and Had are subtypes of EN, which means that a Nor typed value ($|c\rangle$) and a Had typed value ($\frac{1}{\sqrt{2^n}} \otimes_{j=0}^{n-1} (|0\rangle + \alpha(r_j) |1\rangle)$) can be rewritten to an EN typed value. For example, a Had typed value $\frac{1}{\sqrt{2^n}} \otimes_{j=0}^{n-1} (|0\rangle + |1\rangle)$ can be rewritten to an EN type as $\sum_{i=0}^{2^n-1} \frac{1}{\sqrt{2^n}} |i\rangle$. If such a rewrite happens, we correspondingly transform $x[0, n]$'s type to EN in the type environment.

Second, type environment partial order (\leq) and state equivalence (\equiv) also have simultaneity in Figure 13 for local loci, and the relations between loci can be derived based on the following rules, as well as permutations on \uplus operations.

$$\frac{\sigma \leq \sigma'}{\langle \sigma \uplus \sigma_1 \rangle_I \uplus \Sigma \leq \langle \sigma' \uplus \sigma_1 \rangle_I \uplus \Sigma} \qquad \frac{\varphi \leq \varphi'}{\langle \varphi \uplus \varphi_1 \rangle_I \uplus \Phi \leq \langle \varphi' \uplus \varphi_1 \rangle_I \uplus \Phi}$$

Here, we associate a state Φ , with the type environment Σ by sharing the same domain, i.e., $\text{dom}(\Phi) = \text{dom}(\Sigma)$. Thus, the environment rewrites (\leq) happening in Σ gear the state rewrites in Φ . In Figure 13, the rules of environment partial order and state equivalence are one-to-one corresponding. The first three lines describe the properties of reflective, identity, and subtyping equivalence. The fourth line enforces that the environment and state are close under locus permutation. After the equivalence rewrite, the position bases of ranges s_1 and s_2 are mutated by applying the function $q^{|k_1|} \langle |s_1| \times |s_2| \rangle$. One example is the following local locus rewrite from left to right, where we permute the two ranges $x[0, n]$ and $y[0, n]$.

$$\begin{aligned} \{x[0, n] \uplus y[0, n] : \text{EN}\} &\leq \{y[0, n] \uplus x[0, n] : \text{EN}\} \\ \{x[0, n] \uplus y[0, n] : \sum_{i=0}^{2^n-1} \frac{1}{\sqrt{2^n}} |i\rangle |a^i \% N\rangle\} &\equiv \{y[0, n] \uplus x[0, n] : \sum_{i=0}^{2^n-1} \frac{1}{\sqrt{2^n}} |a^i \% N\rangle |i\rangle\} \end{aligned}$$

The last two lines in Figures 13a and 13b describe locus joins and splits, where the latter is an inverse of the former but much harder to perform practically. In the most general form, joining two EN-type states computes the Cartesian product of their basis-kets, shown in the bottom of Figure 13; such operations are computational expensive in verification and validation. Fortunately, the join operations in most quantum algorithms are between a Nor/Had typed and an EN-typed state, Joining a Nor-typed and EN-typed state puts extra qubits in the right location in every basis-ket of the EN-typed state.

⁴The former is a Cartesian product; the latter is \geq NP-hard.

B DisQ Kind Checking

$$\begin{array}{c}
\frac{\Omega(l)(x) = C}{\Omega \vdash_l x : \Omega(l)(x)} \qquad \frac{\Omega \vdash a_1 : C \quad \Omega \vdash_l a_2 : C}{\Omega \vdash_l a_1 + a_2 : C} \qquad \frac{\Omega \vdash a_1 : C \quad \Omega \vdash_l a_2 : C}{\Omega \vdash_l a_1 \cdot a_2 : C} \\
\\
\frac{\Omega \vdash a_1 : C \quad \Omega \vdash_l a_2 : C}{\Omega \vdash_l a_1 = a_2 : C} \qquad \frac{\Omega \vdash a_1 : C \quad \Omega \vdash_l a_2 : C}{\Omega \vdash_l a_1 < a_2 : C} \qquad \frac{\Omega \vdash b : C}{\Omega \vdash \neg b : C}
\end{array}$$

Fig. 15. Arith and Bool Kind Checking

The kind checking procedure $\Omega \vdash_l - : C$ verifies if $-$ is a C kind term, based on the kind checking in [Li et al. 2024], and the rules for arithmetic and Boolean expressions are in Figure 15. The construct $-$ here refers to arithmetic, Boolean equations, or a statement.

C Well-formedness

The correctness of our type system in Section 4.3 is assumed to have well-formed domains below.

Definition C.1 (Well-formed locus domain). The domain of a environment Σ (or state Φ) is *well-formed*, written as $\Omega \vdash \text{dom}(\Sigma)$ (or $\text{dom}(\Phi)$), iff for every locus $\kappa \in \text{dom}(\Sigma)$ (or $\text{dom}(\Phi)$):

- K is disjoint unioned, for every two ranges $\langle x[i, j] \rangle_l$ and $\langle y[i', j'] \rangle_l$ in K , $x[i, j] \cap y[i', j'] = \emptyset$.
- For every range $\langle x[i, j] \rangle_l \in K$, $\Omega(l)(x) = Q(n)$ and $[i, j] \subseteq [0, n]$.

Besides well-formed domain definition, we also require that states (Φ) being well-formed ($\Omega; \Sigma \vdash \Phi$), defined as follows. Here, we use $\Sigma(K)$ and $\Phi(K)$ to find the corresponding state entry pointed to by a locus K' , such that there exists $K_1 . K' = K \boxplus K_1$.

Definition C.2 (Well-formed DisQ state). A state Φ is *well-formed*, written as $\Omega; \Sigma \vdash \Phi$, iff $\text{dom}(\Sigma) = \text{dom}(\Phi)$, $\Omega \vdash \text{dom}(\Sigma)$ (all variables in Φ are in Ω), and:

- For every $K \in \text{dom}(\Sigma)$, s.t. $\Sigma(K) = \text{Nor}$, $\Phi(K) = z|c\rangle(|\beta\rangle)$ and $|\kappa| = |c|$ and $|z| \leq 1$; specifically, if $g = C$, $\beta = \emptyset$ and $|z| = 1$.⁵
- For every $K \in \text{dom}(\Sigma)$, s.t. $\Sigma(K) = \text{Had}$, $\Phi(K) = \frac{1}{\sqrt{2^n}} \otimes_{j=0}^{n-1} (|0\rangle + \alpha(r_j)|1\rangle)$ and $|K| = n$.
- For every $K \in \text{dom}(\Sigma)$, s.t. $\Sigma(K) = \text{EN}$, $\Phi(K) = \sum_{j=0}^m z_j |c_j\rangle(|\beta_j\rangle)$, and for all j , $|K| = |c_j|$ and $\sum_{j=0}^m |z|^2 \leq 1$; specifically, if $g = C$, for all j , $\beta_j = \emptyset$ and $\sum_{j=0}^m |z|^2 = 1$.

D More Case Studies

We provide more case studies here.

D.1 Quantum Teleportation For Ensuring Entanglement Information

Quantum teleportation is a quantum network protocol that teleports information about a qubit to remote locations. This section shows a general use of quantum teleportation to teleport entanglement information. A key observation is that quantum entanglement is also a piece of information; thus, when teleporting a qubit, the possible entanglement associated with the qubit should also be kept by remote qubits.

To demonstrate the case, we use the processes in Example 3.1, as a membrane structure shown in Example D.1 to teleport a qubit $x[1]$ – currently entangles with $x[0]$ – from membrane l to r . The program first creates a shared quantum channel between the two membranes, referred to by $\langle c[0] \rangle_l$

⁵ $|K|$ and $|c|$ are the lengths of K and c , and $|z|$ is the norm.

and $\langle c[0] \rangle_r$, and then teleport $x[1]$ to membrane r to store the information in $\langle c[0] \rangle_r$. The result should show that the entanglement between $x[0]$ and $x[1]$ is transferred to be an entanglement between $x[0]$ and $\langle c[0] \rangle_r$.

Example D.1 (Quantum Teleportation Entanglement Preservation). The example has two membranes. The program code of membrane l is: $\partial c(1) . \{Te(x[1].c[0])\}_l$, and The program code of membrane r is: $\partial c(1) . \{Rt(c[0])\}_r$.

Membrane l has initially two qubit entangled state $x[0, 2] : z_0 |00\rangle + z_1 |11\rangle$. K_c and K_e are:

$$K_c = \langle c[0] \rangle_l \boxplus \langle c[0] \rangle_r \quad K_e = \langle x[0, 2] \boxplus c[0] \rangle_l \boxplus \langle c[0] \rangle_r$$

The following provides the first few transition steps, where $\neg b$ is the bit-flip of the bit b . The R process in steps (3) and (4) refers to $R = b_1 \leftarrow \mathcal{M}^i(x[1]) . b_2 \leftarrow \mathcal{M}^i(c[0]) . a!b_1 . a!2 . 0$.

- (1) $(\{\langle x[0, 2] \rangle_l : \sum_{b=0}^1 z_b |bb\rangle\}, \partial c(1) . \{Te(x[1].c[0])\}_l, \partial c(1) . \{Rt(c[0])\}_r)$
- (2) $\xrightarrow{l.r.1} (\{\langle x[0, 2] \rangle_l : \sum_{b=0}^1 z_b |bb\rangle, K_c : \frac{1}{\sqrt{2}} \sum_{b=0}^1 |bb\rangle\}, \{Te(x[1].c[0])\}_l, \{Rt(c[0])\}_r)$
- (3) $\xrightarrow{l.1} (\{K_e : \sum_{b=0}^1 \frac{1}{\sqrt{2}} z_0 |00\rangle |bb\rangle + \frac{1}{\sqrt{2}} z_1 |11\rangle |(-b)b\rangle\}, \{x[1] \leftarrow H.R\}_l, \{Rt(c[0])\}_r)$
- (4) $\xrightarrow{l.1} (\{K_e : \sum_{b=0}^1 \frac{1}{2} z_0 |0\rangle |0\rangle |bb\rangle + \frac{1}{2} z_0 |0\rangle |1\rangle |bb\rangle + \frac{1}{2} z_1 |1\rangle |0\rangle |(-b)b\rangle - \frac{1}{2} z_1 |1\rangle |1\rangle |(-b)b\rangle\}, \{R\}_l, \{Rt(c[0])\}_r)$

In the above example, the system chooses to let membrane l proceed and perform two transition steps, by applying a CX and H gate operations to the loci $x[1] \boxplus c[0]$ and $x[1]$, and the transitions result in a quantum state at the line (4). Except for the first label, $l.r.1$, all other labels show a choice of l , referring to the nondeterministic choice of picking membrane l in the transition. The probabilities are labeled 1 in all these l choices since there is only one process choice in the membrane. Certainly, membrane choice is nondeterministic, and one can make the wrong choice, e.g., in line (3), instead of choosing membrane l to make a move, membrane r can perform the move. Its prefixed action is waiting for a message that is unavailable. In such a case, membrane r can wait for membrane l to perform a move, or it can perform rule S-REV to reverse the process and release the airlock.

After the transitions, process R in membrane l performs two measurements \mathcal{M}^i (the i flag refers to that the measurement does not count as marking sequence points) on the qubits $x[1]$ and $\langle c[0] \rangle_l$. The measurements have four possibilities, referring to the four possible ways of combining the two outcome bits for the two qubits. The final outcome of the four possibilities is the same. Below, we show the transitions of one of the possibilities by probabilistically choosing the measurement outputs of the two qubits to be 1. Here, $K'_e = \langle x[0] \boxplus c[0] \rangle_l \boxplus \langle c[0] \rangle_r$.

- (5) $\xrightarrow{l.1.\frac{1}{2}} (\{K'_e : \sum_{b=0}^1 \frac{1}{\sqrt{2}} z_0 |0\rangle |bb\rangle - \frac{1}{\sqrt{2}} z_1 |1\rangle |(-b)b\rangle\}, \{w \leftarrow \mathcal{M}^i(c[0]) . a!1 . a!b_2 . 0\}_l, \{T\}_r)$
- (6) $\xrightarrow{l.1.\frac{1}{2}} (\{\langle x[0] \rangle_l \boxplus \langle c[0] \rangle_r : z_0 |0\rangle |1\rangle - z_1 |1\rangle |0\rangle\}, \{a!1 . a!1 . 0\}_l, \{T\}_r)$

The above shows the transitions for the two measurement operations in membrane l . Line (5) performs the first measurement. As the process R in Example D.1 measures $x[1]$ and assigns the bit value to b_1 , which is 1 here. After the transition, every b_1 occurrence is replaced by 1 in the process. The probability of the measurement is $\frac{1}{2}$, which is computed by a geometric sum of all the basis-kets $(\frac{1}{\sqrt{2}} z_0 |0\rangle |1\rangle |bb\rangle$ and $-\frac{1}{\sqrt{2}} z_1 |1\rangle |1\rangle |(-b)b\rangle$ for $b = 0$ or $b = 1$) where $x[1]$'s position basis is $|1\rangle$. Line (6) repeats the process of lines (5), but for measuring $\langle c[0] \rangle_l$ and assigning b_2 to 1. In this procedure, $\langle c[0] \rangle_l$'s position basis is $|b\rangle$ for the basis-kets $\frac{1}{\sqrt{2}} z_0 |0\rangle |bb\rangle$ and $|(-b)\rangle$ for the basis-kets $-\frac{1}{\sqrt{2}} z_1 |1\rangle |(-b)b\rangle$, with $b = 0$ or $b = 1$. Measuring out 1 means that we left with $z_0 |0\rangle |1\rangle$ for the first group by setting b to 1, and $-z_1 |1\rangle |0\rangle$ for the second group by setting $\neg b$ to 1; the combination of the two basis-kets is the resulting state at line (6). In the procedure, the

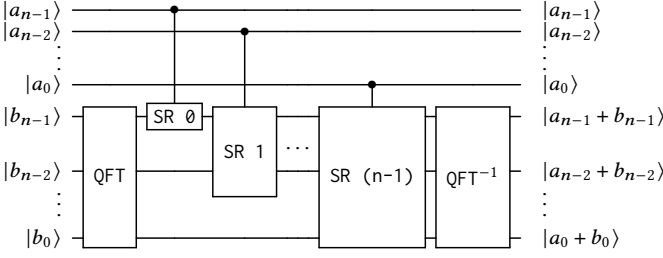


Fig. 16. Quantum QFT-Based Adder Circuit

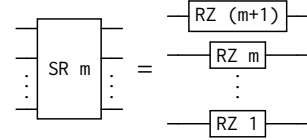


Fig. 17. SR unfolds to many RZ gates.

multiplication of the probabilities along the path of the transitions results in $\frac{1}{4}$, complying with the probability of measuring out two 1s for the $x[1]$ and $\langle c[0] \rangle_l$.

$$(7) \xrightarrow{l,1} (\{\langle x[0] \rangle_l \sqcup \langle c[0] \rangle_r : z_0 |0\rangle |1\rangle - z_1 |1\rangle |0\rangle\}, (a!1. a!1.0) \{\emptyset\}_l, \{T\}_r)$$

$$(8) \xrightarrow{r,1} (\{\langle x[0] \rangle_l \sqcup \langle c[0] \rangle_r : z_0 |0\rangle |1\rangle - z_1 |1\rangle |0\rangle\}, (a!1. a!1.0) \{\emptyset\}_l, T\{\emptyset\}_r)$$

...

$$(9) \xrightarrow{l,r,1} (\{\langle x[0] \rangle_l \sqcup \langle c[0] \rangle_r : z_0 |0\rangle |1\rangle - z_1 |1\rangle |0\rangle\}, \{a!1.0\}_l, \{a?(w).c[0] \leftarrow Z. \text{if } (w) \{c[0] \leftarrow X\}.0\}_r)$$

$$(10) \xrightarrow{l,1} (\{\langle x[0] \rangle_l \sqcup \langle c[0] \rangle_r : z_0 |0\rangle |1\rangle - z_1 |1\rangle |0\rangle\}, (a!1.0) \{\emptyset\}_l, \{a?(w).c[0] \leftarrow Z. \text{if } (w) \{c[0] \leftarrow X\}.0\}_r)$$

$$(11) \xrightarrow{r,1} (\{\langle x[0] \rangle_l \sqcup \langle c[0] \rangle_r : z_0 |0\rangle |1\rangle - z_1 |1\rangle |0\rangle\}, (a!1.0) \{\emptyset\}_l, a?(w).c[0] \leftarrow Z. \text{if } (w) \{c[0] \leftarrow X\}.0 \{\emptyset\}_r)$$

...

$$(12) \xrightarrow{l,r,1} (\{\langle x[0] \rangle_l \sqcup \langle c[0] \rangle_r : z_0 |0\rangle |1\rangle - z_1 |1\rangle |0\rangle\}, \{0\}_l, \{c[0] \leftarrow Z. c[0] \leftarrow X.0\}_r)$$

$$(13) \xrightarrow{r,1} (\{\langle x[0] \rangle_l \sqcup \langle c[0] \rangle_r : z_0 |0\rangle |1\rangle + z_1 |1\rangle |0\rangle\}, \{0\}_l, \{c[0] \leftarrow X.0\}_r)$$

$$(14) \xrightarrow{r,1} (\{\langle x[0] \rangle_l \sqcup \langle c[0] \rangle_r : z_0 |0\rangle |0\rangle + z_1 |1\rangle |1\rangle\}, \{0\}_l, \{0\}_r)$$

The above transitions show the last few steps of evaluating Example D.1. In lines (7) to (12), we transmit two classical bits from membrane l to r through classical message passing. In messaging passing each bit, we first nondeterministically choose to airlock the two membranes through two applications of rule S-MEM, as steps (7) and (8). Since each membrane contains only one process, the probabilities of the choices are 1. We then perform the message communication by rule S-COMM to transmit a message from membrane l to r . Since the choices have been made in (7) and (8), the probability in (9) is 1. Lines (13) and (14) apply two gates to restore the qubit state of $x[1]$ in the new qubit $\langle c[0] \rangle_r$. After the transitions, the entanglement information is transferred from $x[1]$ to $\langle c[0] \rangle_r$, as it is entangled with $x[0]$ now.

D.2 Distributed QFT Adder

A QFT-based adder (Figure 16) performs addition differently than a ripple-carry adder. It usually comes with two qubit arrays y and u , tries to sum the y bits into the u array, by first transforming u 's qubits to QFT-basis and performing addition in the basis, i.e., instead of performing bit arithmetic in a ripple-carry adder, it records addition results via phase rotations. The final inverted QFT operation QFT^{-1} transforms the addition result in the qubit phase back to basis vectors. We show the distributed version of a QFT-adder below, which has a different way of distribution than the ripple-carry adder above.

Example D.2 (Distributed QFT Adder). We define the adder as the membrane definition below. Membrane l holds qubit array x and membrane r takes care of qubit array y , and they share two

n -qubit quantum channels c and c' . C-SR(j) is the controlled SR operation, where $c[j] \boxplus y[0, n] \leftarrow$ C-SR(j) means controlling over $c[j]$ on applying SR to the $y[0, n]$ range.

Recursive Combinator:

$$Rec(j, n, f) = \text{if } (j = n) \ 0 \ \text{else } f(j) \cdot Rec(j+1)$$

Process Definitions:

$$\begin{aligned} Se(j) &= Te(x[j], c[j]) \cdot Rt(c'[j]) & SeR(n) &= Rec(0, n, Se) \\ Re(j) &= Rt(c[j]) \cdot c[j] \boxplus y[0, n] \leftarrow \text{C-SR}(j) \cdot Te(c[j], c'[j]) & ReR(n) &= Rec(0, n, Re) \end{aligned}$$

Membrane Definition:

$$\partial c(n) \cdot \partial c'(n) \cdot \{\{SeR(n)\}\}_l, \partial c(n) \cdot \partial c'(n) \cdot \{y[0, n] \leftarrow \text{QFT} \cdot ReR(n) \cdot y[0, n] \leftarrow \text{QFT}^{-1} \cdot 0\}_r$$

In the above example, after the two n -qubit quantum channel (c and c') are created, membrane r transforms qubit array y to be in QFT-basis. The loop in membrane l sends a qubit in the x array at a time to membrane r via a single qubit quantum channel in c . In the j -th iteration, membrane r receives the information in the qubit $x[j]$, stored in $\langle c[j] \rangle_r$, and applies a C-SR operation that controls over the qubit $\langle c[j] \rangle_r$ on applying SR operation on the y qubit array. Assume that the qubit state in $x[j]$ is $|d_j\rangle$ ($d_j = 0$ or $d_j = 1$), the controlled SR operation adds $2^j * d_j$ to array y 's phase by performing a series of RZ rotations. Then, we teleport $c[j]$ back to membrane l via another single qubit quantum channel in c' . After the loop, we apply an inversed QFT gate to transform the addition result in y 's phase back to its basis vectors.

In each integration, after membrane l teleports qubit $x[j]$ to membrane r , as well as membrane r teleports qubit $c[j]$ to $c'[j]$ in membrane l , the $x[j]$ and $c[j]$ qubits are destroyed, so the qubit numbers in membranes l and r are always less than n and $n+1$, respectively.

D.3 Hidden Subgroup Transitions

We show the transitions below. We have the following process variables for presentation.

$$R' = x[0, n] \boxplus y[0] \leftarrow x < m @ y[0] \cdot R'' \quad R'' = v \leftarrow \mathcal{M}^i(y[0]) \cdot \text{if } (v) \ R \ \text{else } T$$

$$(\emptyset, \{\{R\}\}_l, \{\{T'\}\}_r)$$

- (1) $\xrightarrow{L.1} (\{\langle x[0, n] \rangle_l : |\bar{0}\rangle\}, \{v y(1) \cdot x[0, n] \leftarrow \text{H} \cdot R'\}_l, \{\{T'\}\}_r)$
- (2) $\xrightarrow{L.1} (\{\langle x[0, n] \rangle_l : |\bar{0}\rangle, \langle y[0] \rangle_l : |0\rangle\}, \{x[0, n] \leftarrow \text{H} \cdot R'\}_l, \{\{T'\}\}_r)$
- (3) $\xrightarrow{L.1} (\{\langle x[0, n] \rangle_l : \frac{1}{\sqrt{2^n}} \sum_{j=0}^{2^n-1} |j\rangle, \langle y[0] \rangle_l : |0\rangle\}, \{x[0, n] \boxplus y[0] \leftarrow x < m @ y[0] \cdot R''\}_l, \{\{T'\}\}_r)$
- (4) $\equiv (\{\langle x[0, n] \rangle_l \boxplus \langle y[0] \rangle_l : \frac{1}{\sqrt{2^n}} \sum_{j=0}^{2^n-1} |j\rangle |0\rangle\}, \{x[0, n] \boxplus y[0] \leftarrow x < m @ y[0] \cdot R''\}_l, \{\{T'\}\}_r)$
- (5) $\xrightarrow{L.1} (\{\langle x[0, n] \rangle_l \boxplus \langle y[0] \rangle_l : \frac{1}{\sqrt{2^n}} \sum_{j=m}^{2^n-1} |j\rangle |0\rangle + \frac{1}{\sqrt{m}} \sum_{j=0}^{2^n} |j\rangle |1\rangle\}, \{R''\}_l, \{\{T'\}\}_r)$
- (6) $\xrightarrow{L. \frac{m}{2^n}} (\{\langle x[0, n] \rangle_l \boxplus \langle y[0] \rangle_l : \frac{1}{\sqrt{2^n-m}} \sum_{j=m}^{2^n-1} |j\rangle |0\rangle + \frac{1}{\sqrt{m}} \sum_{j=0}^m |j\rangle |1\rangle\}, \{\text{if } (1) \ R \ \text{else } T\}_l, \{\{T'\}\}_r)$
- (7) $\xrightarrow{L.1} (\{\langle x[0, n] \rangle_l : \frac{1}{\sqrt{m}} \sum_{j=0}^m |j\rangle\}, \{T\}_l, \{\{T'\}\}_r)$

In the above transitions, steps (1) and (2) create an n qubit array for $x[0, n]$ (as $\langle x[0, n] \rangle_l$) and a single qubit for $y[0]$ (as $\langle y[0] \rangle_l$), and step (3) applies n Hadamard gates to $x[0, n]$, resulting in an n -qubit uniformed superposition.

Step (4) rewrite the two qubit groups together into one as a locus $\langle x[0, n] \boxplus y[0] \rangle_l$. Step (5) applies a quantum oracle operation, i.e., a quantum comparison operator. For every $x[0, n]$'s position basis $|j\rangle$, we check if it is greater than m or not. This step essentially partitions all the superposition basis-kets into two groups labeled by the $+$ operation in step (5). The first group contains basis-kets where $j \geq m$ indicated by $y[0]$'s position basis $|0\rangle$, as well as the second group contains basis-kets where $j < m$ indicated by $y[0]$'s position basis $|q\rangle$. Such a quantum oracle circuit implementation is introduced in Li et al. [2022].

Step (6) applies a partial measurement operation on $y[0]$ in membrane l , with the measurement result 1. This results in the basis-kets in $x[0, n]$ to collapse to the second group described above. Since the total number of different basis-kets in the original uniformed superposition is 2^n and there are m different choices in the second group. This means that the measurement probability is $\frac{m}{2^n}$ for measuring out 1. This also indicates that we also need to normalize the amplitudes in the $x[0, n]$'s remaining state, and the multiplication factor is $\sqrt{\frac{2^n}{m}}$, the square-root of the inverted number of the probability value $\frac{m}{2^n}$. This is why the result state amplitude value is $\sqrt{\frac{2^n}{m}} \cdot \frac{m}{2^n} = \frac{1}{\sqrt{m}}$. The final step above performs a classical conditional.

The above transitions are only one of the possible path. It is possible that T' in membrane r might contain nondeterministic steps for executions. Another possibility is that the measurement in line (5) can measure out 0, which leads to a repetition of the above transitions. This is also the meaning of the repeat-until-success scheme, i.e., we try to generate the correct superposition by conducting measurements, until the correct one appears, indicated by measuring out 1.